AD-A179 605

Final Report

RADAR WAVEFORM SYNTHESIS FOR TARGET IDENTIFICATION

Naval Air Systems Command
Contract No. N00019-84-C-0190

Reporting period
July 31, 1984 to August 31, 1985

Prepared by

Kun-Mu Chen, Principal Investigator

Division of Engineering Research
College of Engineering
Michigan State University
East Lansing, Michigan 48824

87 4 10 10

REPORT DOCUMENTATION PAGE

1a. REPORT SECURITY CLASSIFICATION UNCLASSIFIED	1b. RESTRICTIVE MARKINGS N/A

2a. SECURITY CLASSIFICATION AUTHORITY N/A	3. DISTRIBUTION/AVAILABILITY OF REPORT
2b. DECLASSIFICATION/DOWNGRADING SCHEDULE N/A	Approved for public release; distribution unlimited.

4. PERFORMING ORGANIZATION REPORT NUMBER(S) N/A	5. MONITORING ORGANIZATION REPORT NUMBER(S)

6a. NAME OF PERFORMING ORGANIZATION Division of Engineering Res. Michigan State University	6b. OFFICE SYMBOL (If applicable)	7a. NAME OF MONITORING ORGANIZATION Naval Air Systems Command

6c. ADDRESS (City, State, and ZIP Code) East Lansing, Michigan 48824	7b. ADDRESS (City, State, and ZIP Code) Naval Air Systems Command, AIR-340J Department of the Navy Washington, D.C. 20361

8a. NAME OF FUNDING/SPONSORING ORGANIZATION Naval Air Systems Command	8b. OFFICE SYMBOL (If applicable) NAVAIR	9. PROCUREMENT INSTRUMENT IDENTIFICATION NUMBER N00019-84-C-0190

8c. ADDRESS (City, St and ZIP Code) Naval Air Systems Command, AIR-340J Department of the Navy Washington, D.C. 20361	10. SOURCE OF FUNDING NUMBERS			
	PROGRAM ELEMENT NO.	PROJECT NO.	TASK NO.	WORK UNIT ACCESSION NO

11. TITLE (Include Security Classification)

RADAR WAVEFORM SYNTHESIS FOR TARGET IDENTIFICATION

12. PERSONAL AUTHOR(S)
Chen, Kun-Mu

13a. TYPE OF REPORT Final	13b. TIME COVERED FROM 7/31/84 TO 8/31/85	14. DATE OF REPORT (Year, Month, Day) 9/15/85	15. PAGE COUNT 66

16. SUPPLEMENTARY NOTATION

17.	COSATI CODES		18. SUBJECT TERMS (Continue on reverse if necessary and identify by block number)
FIELD	GROUP	SUB-GROUP	Radar target discrimination and identification, natural frequencies, E-pulses, single-mode extraction signals, discriminant signals

19. ABSTRACT (Continue on reverse if necessary and identify by block number)

The purpose of this research is to develop a new scheme of radar discrimination and identification. The new scheme is based on the natural frequencies of the target. It consists of synthesizing aspect-independent discriminant signals, called Extinction-pulses E-pulses and single-mode extraction signals which, when convolved numerically with the late-time transient response of an expected target, lead to zero or single-mode responses. When the synthesized, discriminant signals for an expected target are convolved with the radar return from a different target, the resulting signal will be significantly different from the expected zero or single-mode responses, thus, the differing targets can be discriminated.

The theory on E-pulses and single-mode extraction signals is outlined based on the time-domain and the frequency-domain analysis. Experimental results on complex targets are given. Some new methods for extracting the natural frequencies of a complex target from its measured pulse response are presented.

20. DISTRIBUTION/AVAILABILITY OF ABSTRACT ☒ UNCLASSIFIED/UNLIMITED ☐ SAME AS RPT ☐ DTIC USERS	21. ABSTRACT SECURITY CLASSIFICATION UNCLASSIFIED
22a. NAME OF RESPONSIBLE INDIVIDUAL Barry Dillon	22b. TELEPHONE (Include Area Code) (202) 692-7415 · 22c. OFFICE SYMBOL NAVAIR

DD FORM 1473, 84 MAR   83 APR edition may be used until exhausted   SECURITY CLASSIFICATION OF THIS PAGE
All other editions are obsolete

UNCLASSIFIED

Table of Contents

1. Introduction

This is the final report on the research program on "Radar Waveform Synthesis for Target Identification" supported by the Naval Air Systems Command under Contract N00019-84-C-0190, and it reports the progress for the period of July 31, 1984 to August 31, 1985.

The purpose of this research is to develop a new scheme of radar discrimination and identification. The new scheme is based on the natural frequencies of the target. It consists of synthesizing aspect-independent discriminant signals, called Extinction-pulses (E-pulses*) and single-mode extraction signals which, when convolved numerically with the late-time transient response of an expected target, lead to zero or single-mode responses. When the synthesized, discriminant signals for an expected target are convolved with the radar return from a different target, the resulting signal will be significantly different from the expected zero or single-mode responses, thus, the differing targets can be discriminated.

The complex natural resonant frequencies of a radar target are aspect independent features of its transient electromagnetic response. A number of researchers have recently attempted to discriminate among various targets by extracting those natural frequencies from late-time transient radar returns. Since extraction of natural frequencies from late-time target responses is an inherently ill-conditioned numerical procedure, very large S-N ratios are required in the transient return. It has therefore been concluded that this method for the direct discrimination of differing target is impractical.

---

*The E-pulse is similar to the K-pulse studied by other workers [1-2].

1

Our discrimination scheme differs significantly. Synthesis of the discriminant signals requires only knowledge of the natural frequencies of various expected targets. The latter natural frequencies are measured in the laboratory where they are extracted from the late-time pulse responses of target scale models. The numerically ill-conditioned natural frequency extraction procedure need therefore be applied only to target responses measured in a controlled S-N environment. Synthesized discriminant signals based upon those laboratory measurements are stored as computer data files, and subsequently convolved numerically with actual transient target radar returns. Since the latter convolution operation is numerically well conditioned (a smoothing integral operator), the S-N requirements for the actual radar return are significantly relaxed.

Another observation made in the course of our study is worth noting. It is common thinking among many researchers that radar detection utilizing the late-time transient radar reutrn may not be practical because it contains little energy; most energy is associated with the early-time part of that return. This thinking may be true for very low-Q targets. Fortunately, for most space vehicles, such as rockets and aircrafts, these targets are not exactly low-Q structures. There is sufficient energy contained in the late-time returns of such targets, as can be evidenced from our measured responses of complex targets as discussed in Section 3.

Under the sponsorship of Naval Air Systems Command, the research program has progressed steadily over the past few years and so far we have a good understanding of the basic principle and have demonstrated the feasibility and applicability of our scheme in discriminating between complex radar targets [3-6]. It appears that this scheme has a good potential to be a useful and practical method for radar detection in the future.

In this report we outline the progress made over the past year. In Section 2, the basic theory on E-pulse and single-mode extraction signals is outlined based on the time-domain and the frequency-domain analysis. In Section 3, experimental results of the scheme when applied to complex targets are given. In Section 4, shaping extraction signals by proper choice of basis functions is discussed. In Section 5, new methods for extracting the natural frequencies of a complex target from its measured pulse response are presented. The future plans are given in Section 6. Two recent papers published by us are included in Appendices.

2. Theory on E-Pulses and Single-Mode Extraction Signals

Basic theory on E-pulses and single-mode extraction signals is briefly outlined in this section.

2.1. Time domain analysis

Assume that the measured time-domain scattered field response waveform of a conducting radar target can be written during the late-time period ($t > T_\ell$) as a sum of damped sinusoids

$$r(t) = \sum_{n=1}^{N} a_n e^{\sigma_n t} \cos(\omega_n t + \phi_n) \qquad t > T_\ell \qquad (1)$$

where a_n and ϕ_n are the aspect dependent amplitude and phase of the n'th mode, $s_n = \sigma_n + j\omega_n$ is the aspect independent natural frequency of the n'th mode, and only N modes are assumed to be excited by the incident field waveform. Then, the convolution of an E-pulse waveform $e(t)$ with the measured response waveform becomes

$$c(t) = e(t) * r(t) = \int_0^{T_e} e(t') r(t - t') dt'$$

$$= \sum_{n=1}^{N} a_n e^{\sigma_n t} [A_n \cos(\omega_n t + \phi_n) + B_n \sin(\omega_n t + \phi_n)] \qquad (2)$$

$$\text{for } t > T_L = T_\ell + T_e$$

3

where

$$A_n = \int_0^{T_e} e(t')e^{-\sigma_n t'} \cos\omega_n t' dt'$$
$$B_n = \int_0^{T_e} e(t')e^{-\sigma_n t'} \sin\omega_n t' dt' \qquad (3)$$

and T_e is the finite duration of $e(t)$.

Two interesting waveforms are now considered. Constructing $e(t)$ to result in $c(t) = 0$, $t > T_L$, requires

$$A_n = B_n = 0 \qquad 1 \leq n \leq N \qquad (4)$$

In addition, $e(t)$ can also be constructed so that $c(t)$ is composed of just a single mode. In this case $e(t)$ is termed a "single mode extraction waveform". If the phase of $c(t)$ is unimportant, $e(t)$ can be constructed by demanding

$$A_n = B_n = 0 \qquad 1 \leq n \leq N, \quad n \neq m \qquad (5)$$

to excite the m'th natural mode. On the other hand, requiring

$$A_n = B_n = 0 \qquad 1 \leq n \leq N, \quad n \neq m$$
$$A_m = 0 \qquad (6)$$

results in

$$c(t) = a_m e^{\sigma_m t} B_m \sin(\omega_m t + \phi_m) \qquad (7)$$

and requiring

$$A_n = B_n = 0 \qquad 1 \leq n \leq N, \quad n \neq m$$
$$B_m = 0 \qquad (8)$$

yields

$$c(t) = a_m e^{\sigma_m t} A_m \cos(\omega_m t + \phi_m) \qquad (9)$$

4

The E-pulse resulting from (5) is termed a "sin/cos" single mode extraction waveform, since it excites both sine and cosine components in $c(t)$, while (6) results in a "sine" and (8) in a "cosine" single mode extraction waveform. With the proper normalizations of $e(t)$ (giving $A_m = B_m$), the convolved waveforms (7) and (9) can be combined to yield the frequency of the m'th mode, $s_m = \sigma_m + j\omega_m$.

2.2. Frequency domain analysis

The convolution of the E-pulse waveform with the measured response waveform can also be written in the form

$$c(t) = \sum_{n=1}^{N} a_n |E(s_n)| e^{\sigma_n t} \cos(\omega_n t + \psi_n) \qquad t > T_L \qquad (10)$$

where

$$E(s) = \mathcal{L}\{e(t)\} = \int_0^{T_e} e(t) e^{-st} dt \qquad (11)$$

is the Laplace transform of the E-pulse waveform, and

$$\psi_n = \phi_n + \tan^{-1}\left[-\frac{E_{in}}{E_{rn}}\right] \qquad (12)$$

where

$$E_{in} = \text{Im}\{E(s_n)\} \qquad E_{rn} = \text{Re}\{E(s_n)\} \qquad (13)$$

Now, $c(t) = 0$ for $t > T_L$ requires

$$E_{in} = E_{rn} = 0 \qquad 1 \le n \le N \qquad (14)$$

or, equivalently,

$$E(s_n) = E(s_n^*) = 0 \qquad 1 \le n \le N \qquad (15)$$

In addition, a sin/cos single mode extraction waveform can be constructed via

$$E(s_n) = E(s_n^*) = 0 \qquad 1 \le n \le N, \quad n \ne m \qquad (16)$$

while a sine single mode extraction waveform requires

5

$$E(s_n) = E(s_n^*) = 0 \qquad 1 \leq n \leq N, \quad n \neq m \Big\}$$

$$E(s_m) = -E(s_m^*) \qquad \qquad \Big\} \tag{17}$$

and a cosine single mode extraction waveform requires

$$E(s_n) = E(s_n^*) = 0 \qquad 1 \leq n \leq N, \quad m \neq m \Big\}$$

$$E(s_m) = E(s_m^*) \qquad \qquad \Big\} \tag{18}$$

It is easily shown that the frequency domain and time domain requirements for synthesizing an E-pulse are identical. By expanding the exponential in (11), one can show that (16), (17), and (18) are equivalent to (5), (6), and (8), respectively.

One benefit of using a frequency domain approach comes via the increased intuition allowed by equation (10). When an E-pulse waveform is convolved with the measured response of an unexpected target, the amplitudes of the resulting natural mode components are determined by evaluating the magnitude of the spectrum of $e(t)$ at the natural frequencies of the target (a result of the Cauchy residue theorem). Thus, the E-pulse spectrum becomes the key tool in predicting the success of E-pulse discrimination.

2.3. E-pulse synthesis (using Frequency Domain Analysis)

To implement the E-pulse requirements it becomes necessary to represent the waveform mathematically. Let $e(t)$ be composed of two components

$$e(t) = e^f(t) + e^e(t) \tag{19}$$

Here $e^f(t)$ is a forcing component which excites the target, and $e^e(t)$ is an extinction component which extinguishes the response due to $e^f(t)$. The forcing component is a free choice, while the extinction component is determined by first expanding in a set of basis functions

6

$$e^e(t) = \sum_{m=1}^{M} \alpha_m f_m(t) \tag{20}$$

and then employing the E-pulse conditions. Using (15) results in the matrix equation

$$
\begin{bmatrix}
F_1(s_1) & F_2(s_1) & \cdots & F_M(s_1) \\
& \vdots & & \\
F_1(s_N) & F_2(s_N) & \cdots & F_M(s_N) \\
F_1(s_1^*) & F_2(s_1^*) & \cdots & F_M(s_1^*) \\
& \vdots & & \\
F_1(s_N^*) & F_2(s_N^*) & \cdots & F_M(s_N^*)
\end{bmatrix}
\begin{bmatrix}
\alpha_1 \\
\alpha_2 \\
\\
\vdots \\
\\
\alpha_M
\end{bmatrix}
=
\begin{bmatrix}
-E^f(s_1) \\
\vdots \\
-E^f(s_N) \\
-E^f(s_1^*) \\
\vdots \\
-E^f(s_N^*)
\end{bmatrix}
$$

where

$$\left. \begin{aligned} F_m(s) &= \mathscr{L}\{f_m(t)\} \\ E^f(s) &= \mathscr{L}\{e^f(t)\} \end{aligned} \right\} \tag{22}$$

and $M = 2N$ is chosen to make the matrix square.

Two types of E-pulses are now easily identified. When $e^f(t) \neq 0$, the forcing vector on the right hand side of (21) is nonzero, and solutions for the basis function amplitudes exist for any choice of E-pulse duration, T_e, which does not cause the matrix to be singular. In contrast, when $e^f(t) = 0$ the matrix equation becomes homogeneous, and solutions for $e^e(t)$ exist only for specific durations T_e which are calculated by solving for zeros of the determinantal equation. The former type of E-pulse is termed "forced" and the latter "natural". Since a natural E-pulse has no forcing component, it is viewed as extinguishing its own excited field.

7

A very useful application of the frequency domain approach results from using pulses as the basis functions in (20). Let

$$
f_m(t) = \begin{cases} g(t - [m - 1]\Delta) & (m - 1)\Delta \leq t \leq m\Delta \\ 0 & \text{elsewhere} \end{cases} \tag{23}
$$

where $g(t)$ is an arbitrary function, and Δ is the pulse width. Then

$$
F_m(s) = \int_0^{T_e} g(t - [m - 1]\Delta)e^{-st}dt
$$

$$
= F_1(s)e^{s\Delta}e^{-sm\Delta} \tag{24}
$$

and the matrix equation (21) can be written for the case of the natural E-pulse as

$$
\begin{bmatrix}
1 & Z_1 & Z_1^2 & \cdots & Z_1^{2N-1} \\
\vdots & \vdots & \vdots & & \vdots \\
\vdots & \vdots & \vdots & & \vdots \\
\vdots & \vdots & \vdots & & \vdots \\
1 & Z_N & Z_n^2 & \cdots & Z_N^{2N-1} \\
1 & Z_1^* & (Z_1^*)^2 & \cdots & (Z_1^*)^{2N-1} \\
\vdots & \vdots & \vdots & & \vdots \\
\vdots & \vdots & \vdots & & \vdots \\
\vdots & \vdots & \vdots & & \vdots \\
1 & Z_N^* & (Z_N^*)^2 & \cdots & (Z_N^*)^{2N-1}
\end{bmatrix}
\begin{bmatrix}
\alpha_1 \\
\alpha_2 \\
\\
\\
\vdots \\
\vdots \\
\vdots \\
\\
\\
\alpha_{2N}
\end{bmatrix}
= 0 \tag{25}
$$

where

$$
Z_n = e^{-s_n\Delta} \tag{26}
$$

Equation (25) is homogeneous, and thus has solutions only when the determinant of the matrix is zero. As the determinant is of the Vandermonde type, the condition for a singular matrix can be calculated easily as

$$
\Delta = \frac{p\pi}{\omega_k} \qquad p = 1,2,3,\ldots \qquad 1 \leq k \leq N \tag{27}
$$

Thus, the duration of natural E-pulse depends merely on the imaginary part of one of the natural frequencies. With σ determined, the basis function amplitudes can be calculated using Cramer's rule and the theory of determinants as

$$a_m = (-1)^m P_{(2N-1)-(m-1)} \tag{28}$$

where P_{i-j} is the sum of the products $n - i$ at a time, without repetitions, of the quantities Z_1, Z_1^*, Z_2,...,Z_N^*.

Note that $g(t)$ does not appear in this analysis, and thus the resulting pulse amplitudes are independent of the individual pulse shapes. However, when discriminating between different targets, $g(t)$ manifests quite importantly through the term $F_1(s)$.

The synthesis of single-mode extraction signals can be carried out similarly based on (16), (17) or (18). The only difference from the E-pulse synthesis is that the number of basis functions M should be chosen to match the number of equations presented by (16), (17), or (18).

It is also noted that the E-pulse synthesis based on the time domain analysis has been published recently [3] (see Appendix 1).

3. Experimental Results on Complex Radar Targets

In the preceding section, the E-pulse and single-mode extraction signals were synthesized based on the prior knowledge of target's natural frequencies. In the case of complex radar targets, this information is difficult to obtain, and the synthesis of the discriminant signals can only be carried out by a combined experimental and theoretical technique.

Over the past few years, we have developed the techniques (which can be refined further) for synthesizing the E-pulses and single-mode extraction signals for complex targets based on measured pulse responses of their scale models. Through the convolution of these synthesized discriminant signals with the

9

measured radar responses of the targets, we have definitely demonstrated the capability of our scheme to discriminate between complex targets.

The following steps are used in synthesizing the discriminant signals for the complex targets:

(1) Measure the pulse response of the scale model of the target at various aspect angles.

(2) Use the Fast Fourier Transform to obtain approximate values of natural frequencies from the measured pulse response.

(3) Employ the continuation method [7] and the natural frequencies obtained from FFT as the initial guesses to calculate accurate values of natural frequencies of the target. At each step of the algorithm, the condition number of the regularized problem is checked.

(4) With the natural frequencies of the target determined, the theoretical technique described in Section 2 is then applied to synthesize the discriminant signals.

After the discriminant signals of a complex target were synthesized, they were convolved with the measured radar responses of the target at various aspect angles to check the workability of the scheme.

For the purpose of demonstration, two complex targets, scale models of McDonnel-Douglas F-18 airplane and Boeing 707 airplane which have similar sizes but different geometries, are used here.

Figures 1 and 2 show the measured pulse response of the 707 and the F-17 scale models, respectively. Each model is constructed of aluminum and has a geometry as indicated in the figures. Also shown are the dominant natural frequencies extracted from the late time portion of the response using the continuation method. These frequencies can then be used to construct natural E-pulse and single-mode extraction signals.
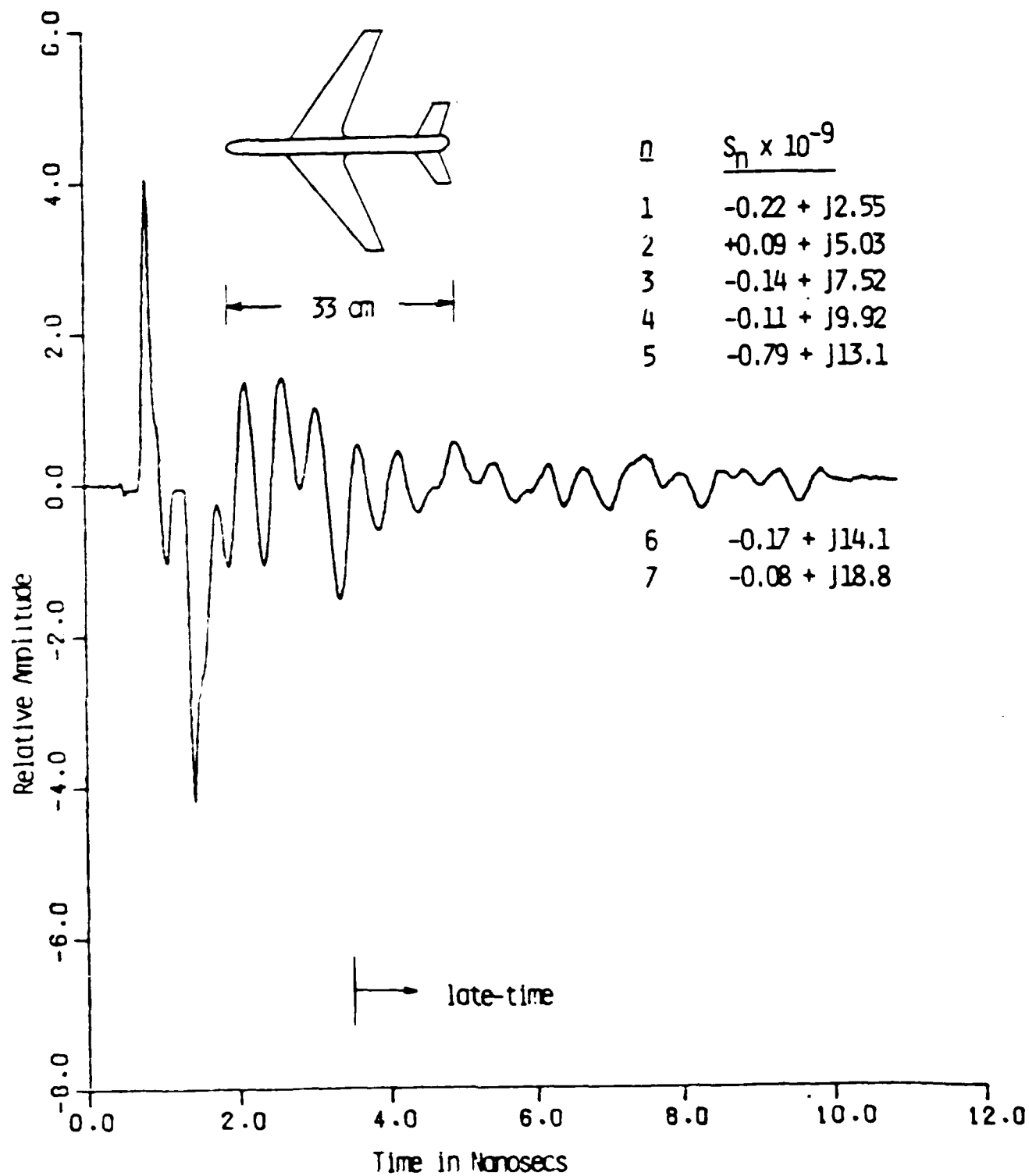
Fig. 1. Measured response of a Boeing 707 aircraft model and seven dominant natural frequencies.
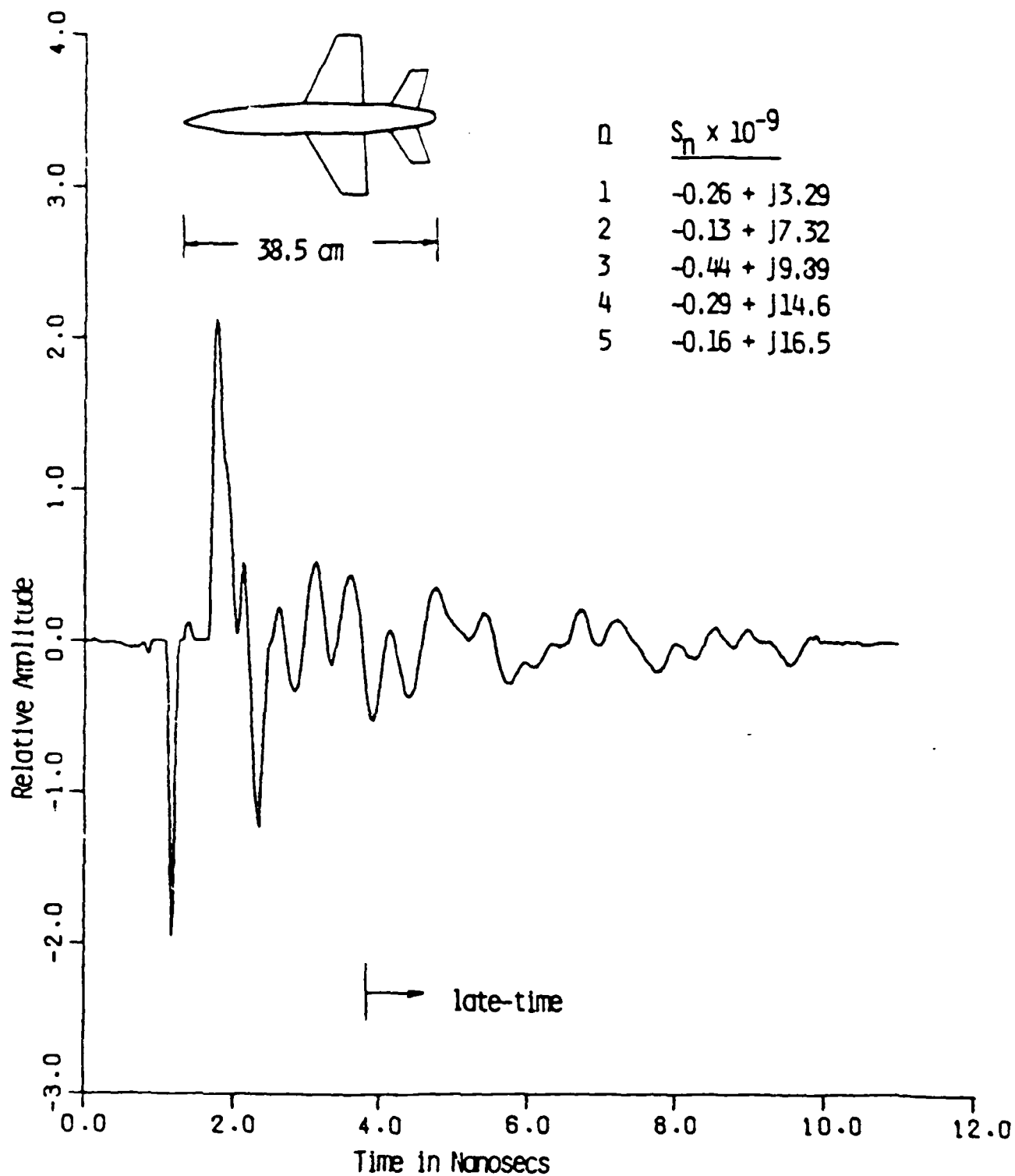
11

Fig. 2. Measured response of a McDonnell Douglas F-18 aircraft model and five dominant natural frequencies.

Pulse basis function natural E-pulses of minimum duration considered for each of the two targets are shown in Figs. 3 and 4. The cosine first-mode and the sine first-mode extraction signals for the 707 airplane are shown in Fig. 5. Other single-mode extraction signals for these two airplanes are not shown here for brevity.

Synthesized E-pulses and single-mode extraction signals for these two airplanes are then convolved with their measured pulse responses shown in Figs. 1 and 2. The convolved results are depicted in the following figures.

Figure 6 shows the convolution of the E-pulse for the F-18 plane with the measured radar response of the F-18 plane. The convolved output shows a strong early-time response followed by a "extinguished" (almost zero) late-time response as expected. Figure 7 shows the convolved output of the E-pulse for the 707 plane with the measured radar response of the F-18 plane. This convolved output shows a significant, "unextinguished" late-time response implying that the 707 E-pulse was convolved with the radar response of a wrong target other than the 707 plane. Figure 8 shows the convolution of the E-pulse for the 707 plane with the measured radar response of the 707 plane. The convolved output shows a nearly "extinguished" late-time response because it is the right target for that E-pulse. Figure 9 indicates the convolved result of the E-pulse for the F-18 plane with the measured radar response of the 707 plane. As expected, the convolved result shows a significant "unextinguished" late-time response. The results of Figs. 6 to 9 clearly show the capability of target discrimination using the E-pulses of the targets.

To enhance the certainty of the target discrimination, the single-mode extraction signals of the target were used to convolve with the measured radar responses of the right target and the wrong targets. Figure 10 shows the convolved results of the measured radar response of the 707 plane with the
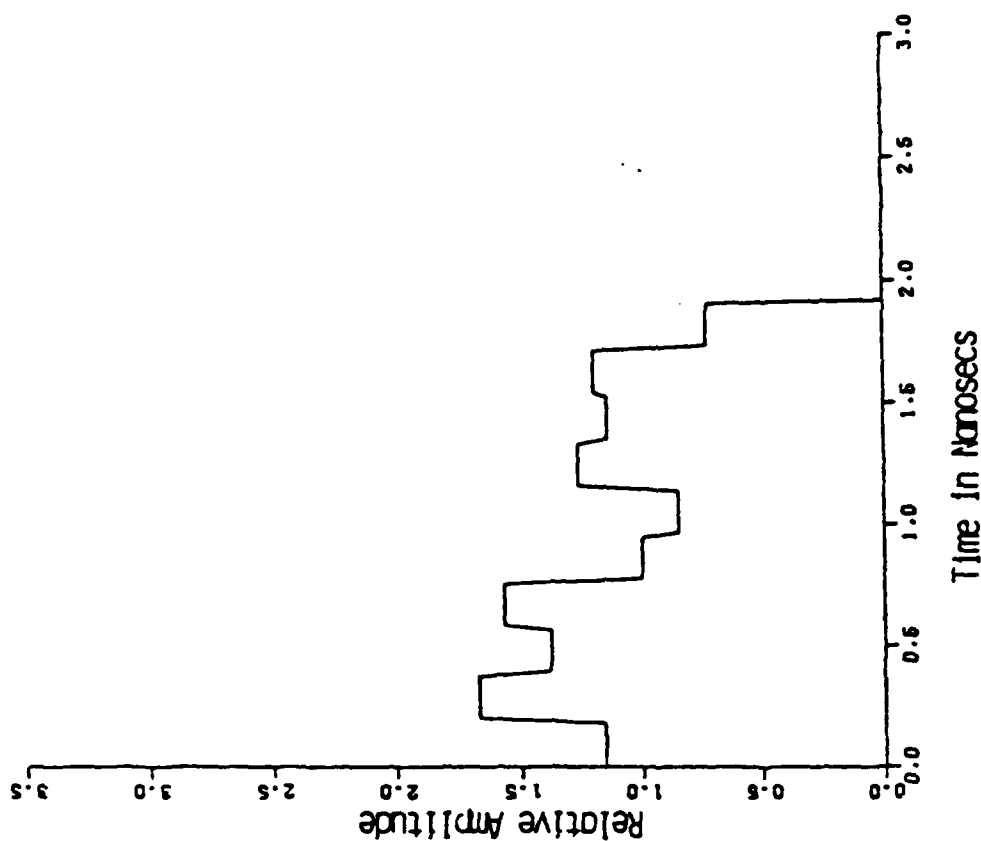
13

Fig. 4. Natural E-pulse constructed to extinguish the five dominant modes in the F-18 measured response.
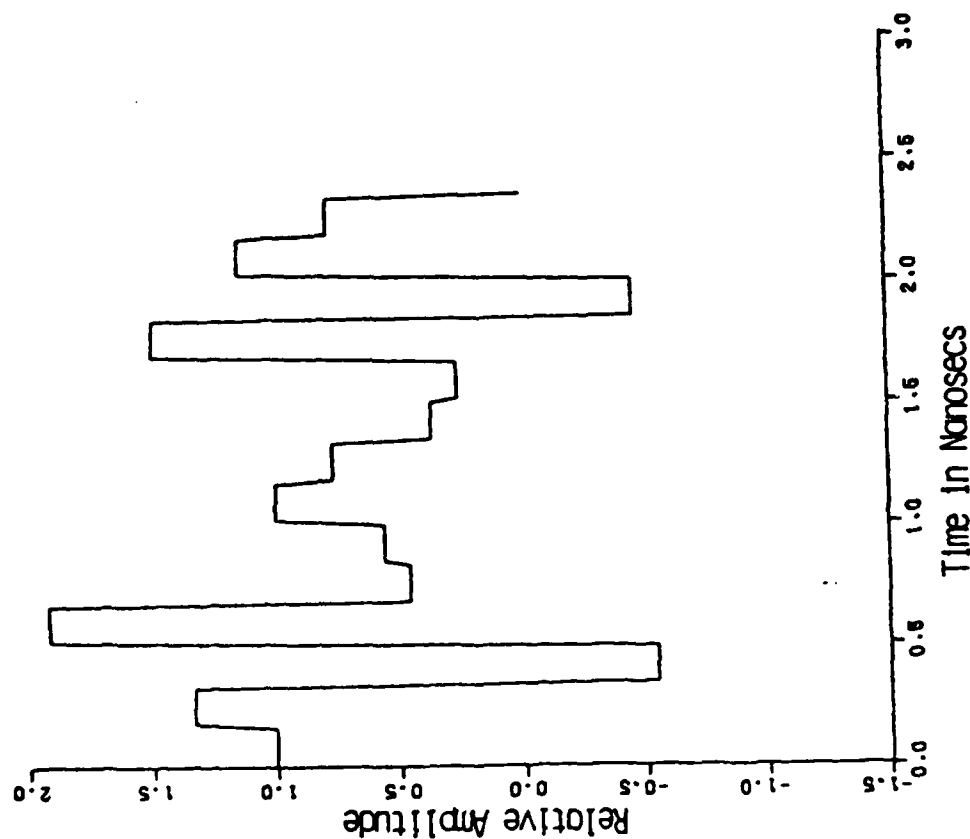

Fig. 3. Natural E-pulse constructed to kill the seven dominant modes in the 707 measured response.
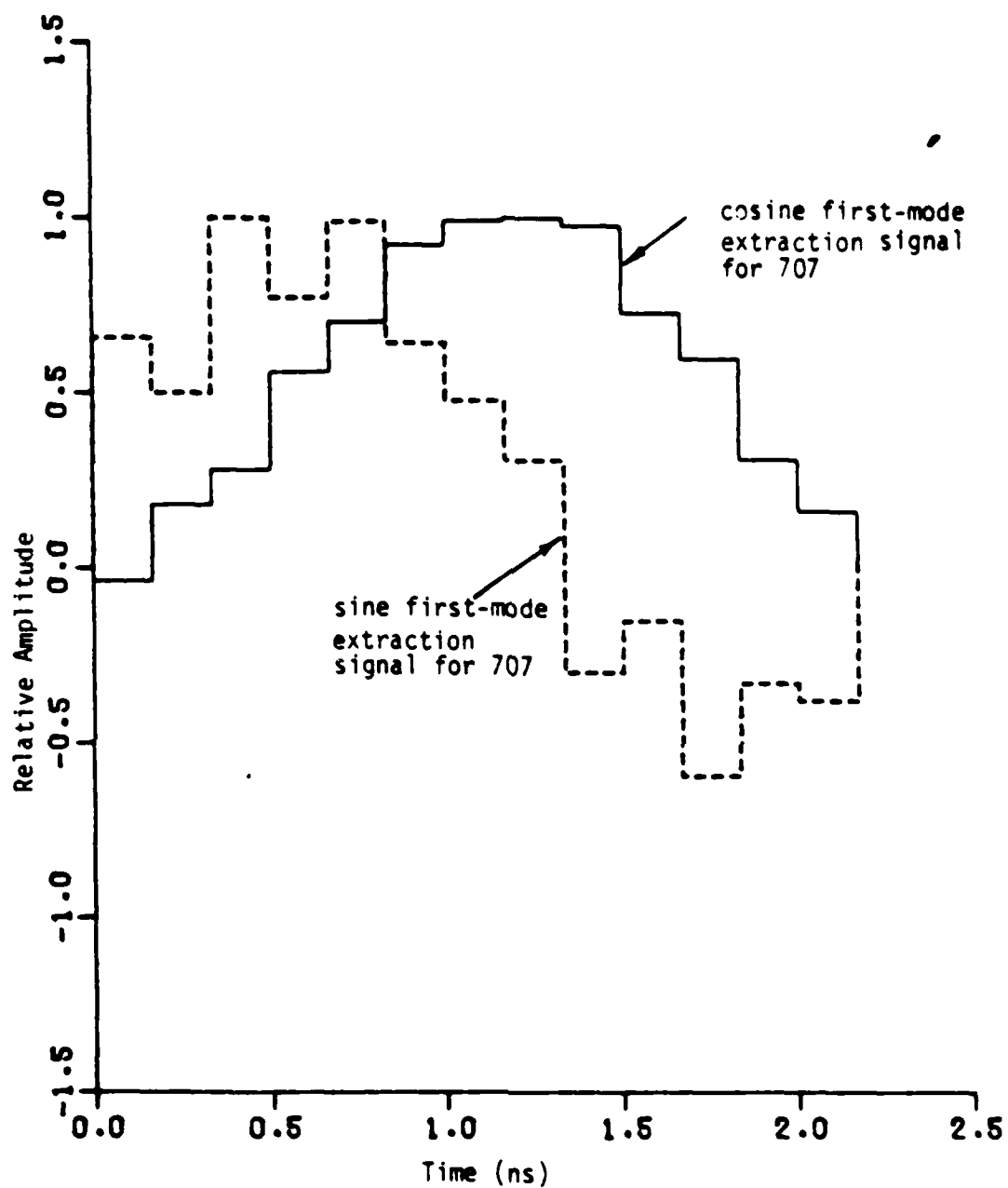
14

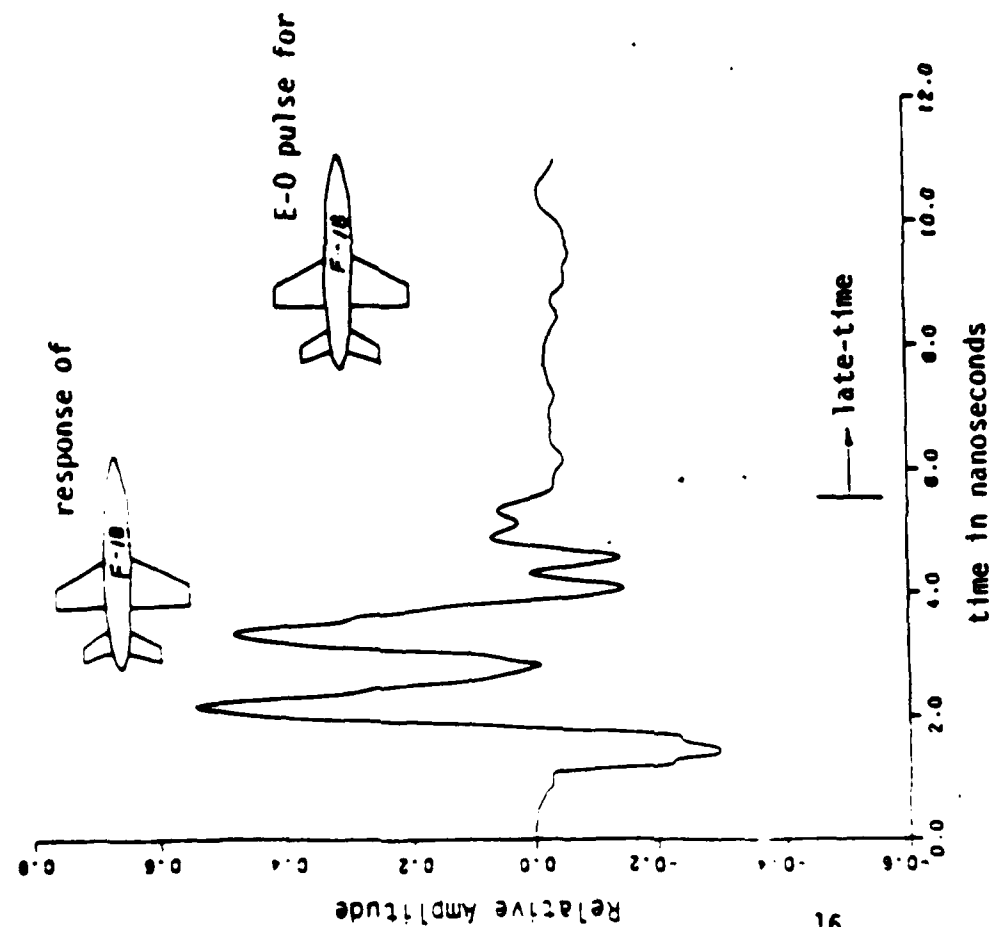Fig. 5. Synthesized first-mode extraction signals for the 707 airplane model.
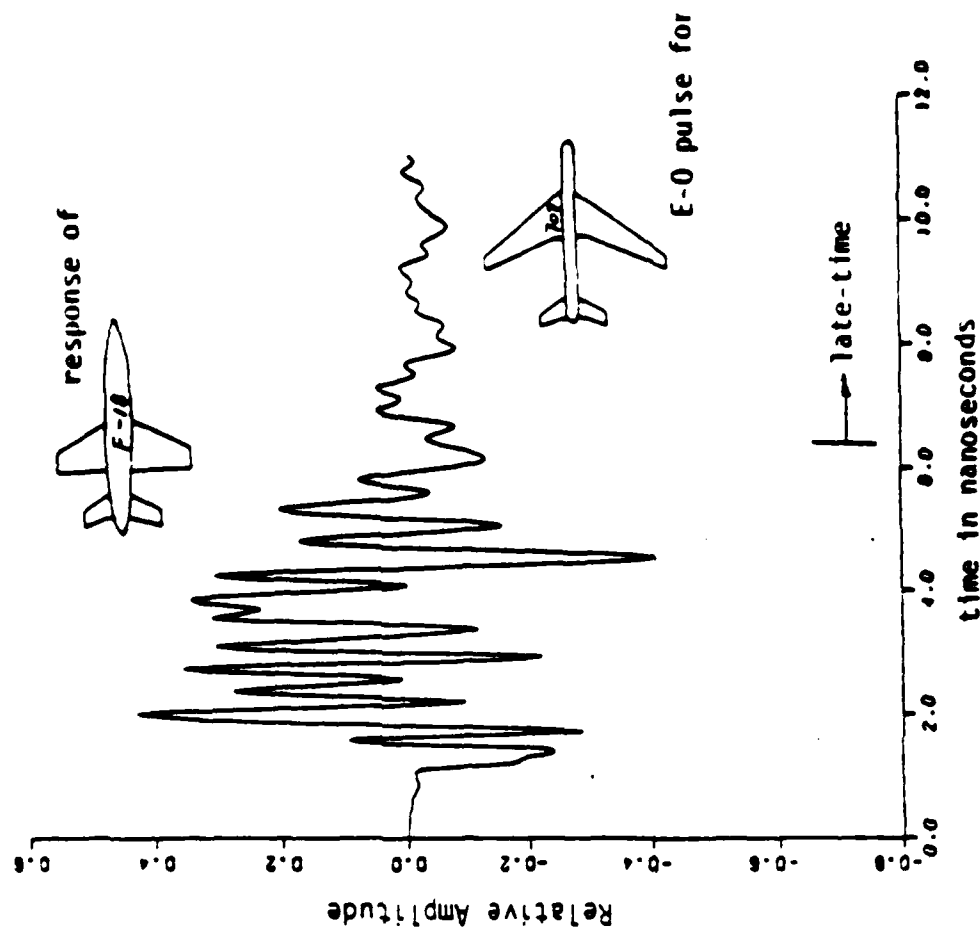
Fig. 7.   Convolution of the 707 E- pulse with the F-18 response showing a significant late-time response.
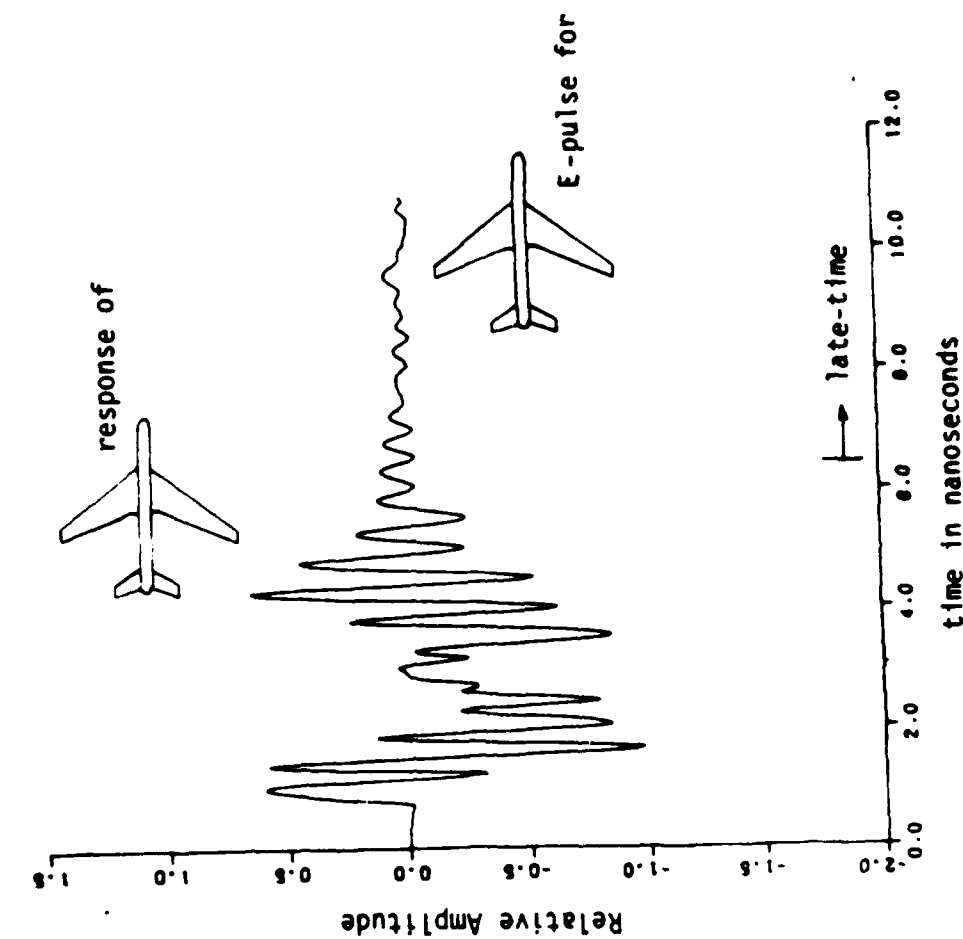

Fig. 6.   Convolution of the F-18 E- pulse with the F-18 measured response showing "extinguished" late-time region.

16

Fig. 9. Convolution of the F-18 E-pulse with the 707 measured response showing a significant late-time response.

Fig. 8. Convolution of the 707 E-pulse with the 707 measured response showing "extinguished" late-time region.
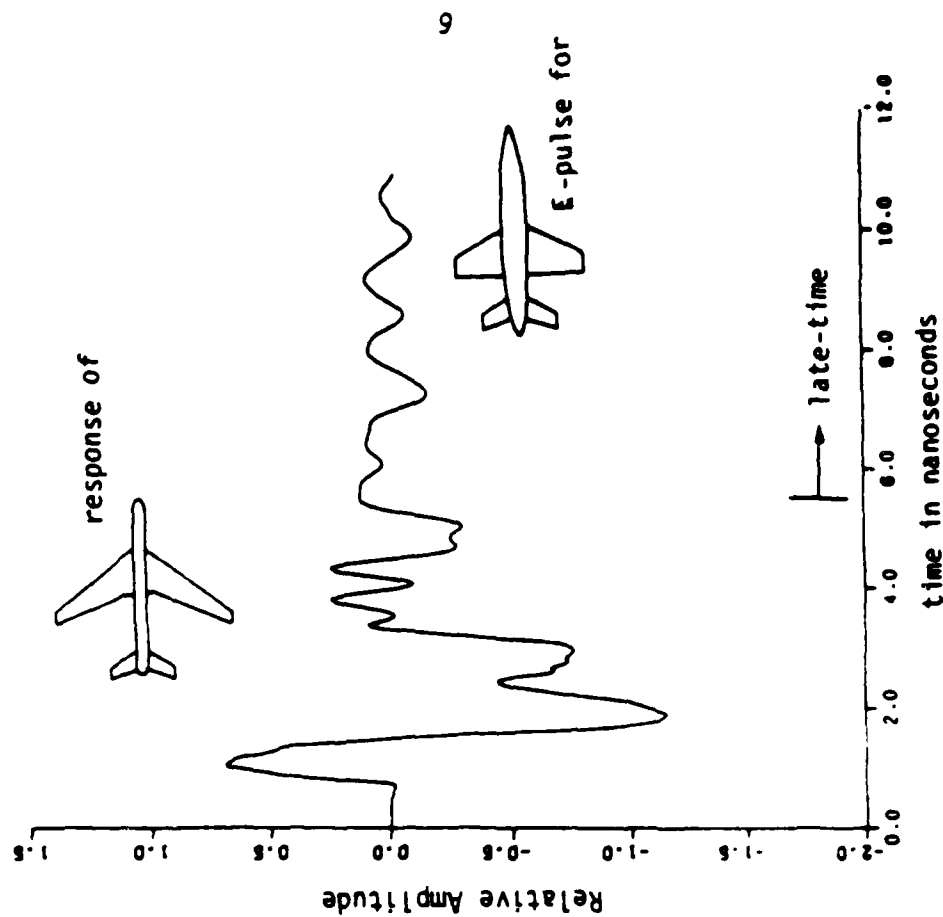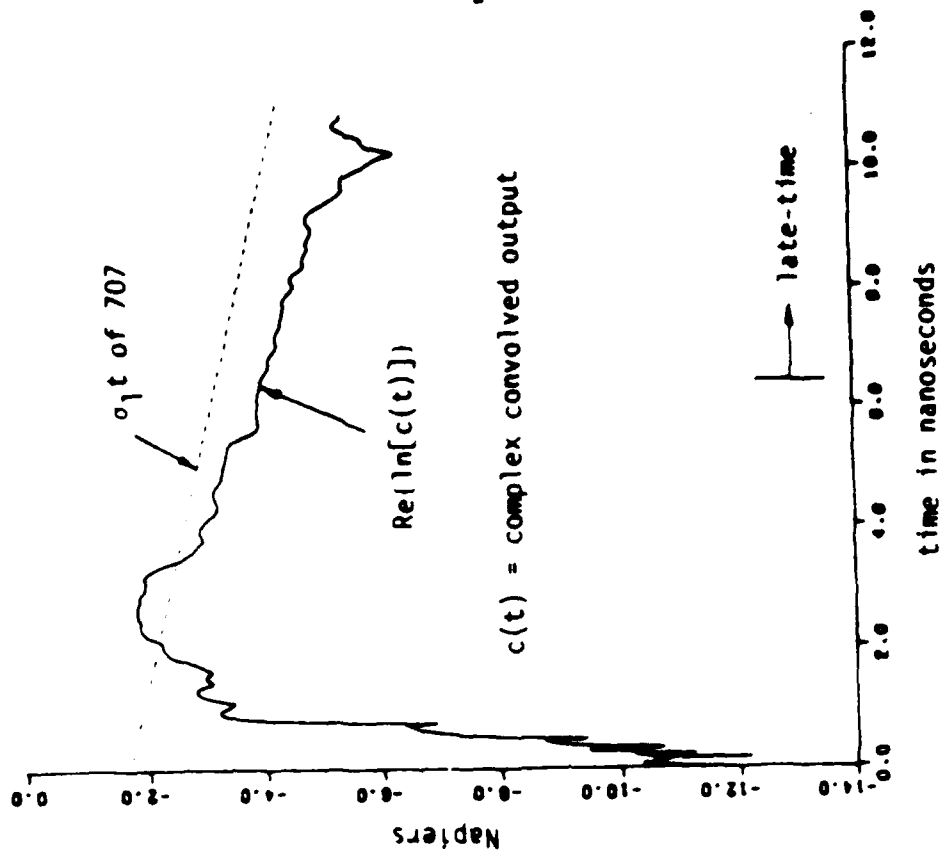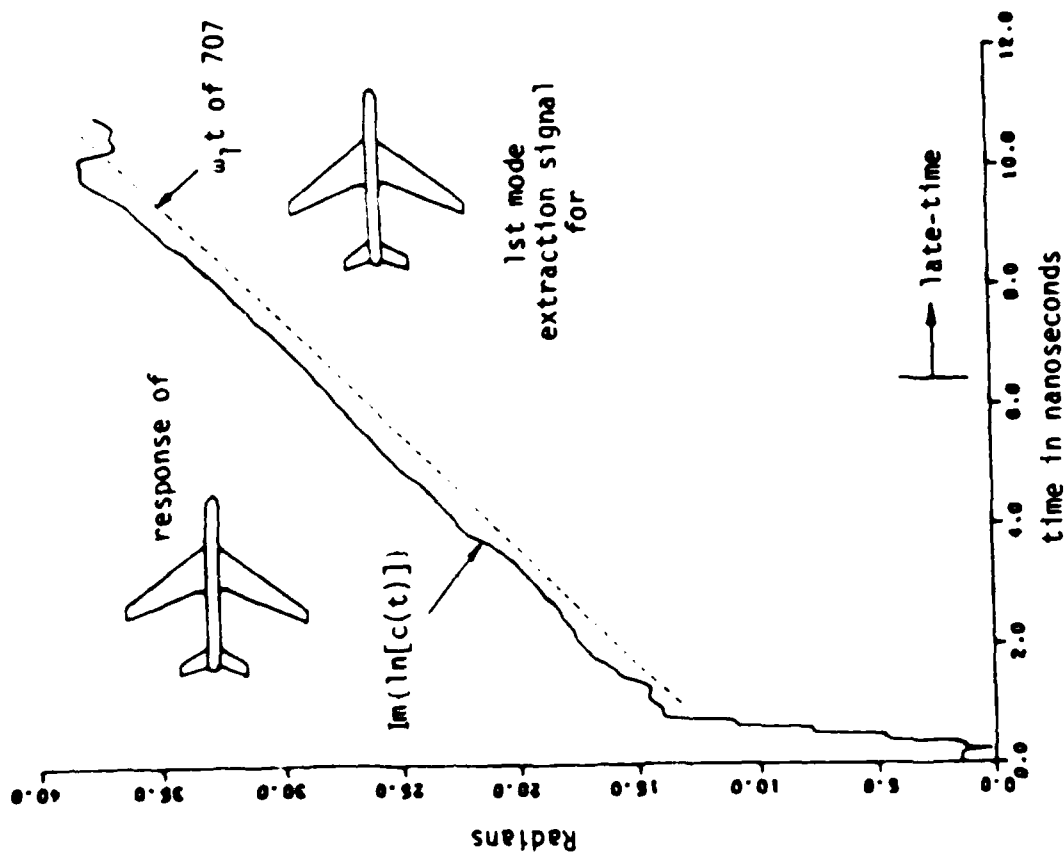
Fig. 10. Angular frequency and damping coefficient extracted from the complex convolved output of the first mode extraction signal for the 707 target and the 707 measured response.

first-mode extraction signal for the 707 plane. The left figure of Fig. 10 shows

the angular frequency line extracted from the complex convolved output. Since

this line is almost parallel to the $\omega_1 t$ line (of the 707) in the late-time

period, it implies that the measured radar response is from the right target of

the 707 plane. The right figure of Fig. 10 shows the damping coefficient line

extracted from the complex convolved output. This line is closely parallel with

the $\sigma_1 t$ line (of the 707) in the late-time period, implying the target is the

707 plane. Figure 11 shows the convolved results of the measured radar response

of the 707 plane with the fourth-mode extraction signal for the 707 plane. In

this figure, the extracted angular frequency line is almost parallel to the

$\omega_4 t$ line (of the 707) and the extracted damping coefficient line closely

parallel to the $\sigma_4 t$ line (of the 707) in the late-time period. This implies

that the radar response belongs to the right target of the 707 plane. When the

measured response of the F-18 plane is convolved with the first-mode extraction

signal of the 707 plane, the results are shown in Fig. 12. The extracted angular

frequency line is not parallel to the $\omega_1 t$ line (of the 707) and the extracted

damping coefficient line deviates from the $\sigma_1 t$ line (of the 707) in the late-

time period. This indicates that the measured radar response comes from a

wrong target other than the 707 plane. Figure 13 shows the convolved results of

the measured radar response of the F-18 plane with the fourth-mode extraction

signal of the 707 plane. The extracted angular frequency line and the damping

coefficient line deviate from the $\omega_4 t$ line (of the 707) and the $\sigma_4 t$ line (of the

707), respectively, in the late-time period, implying that the radar response

belongs to a wrong target other than the 707 plane.

Results depicted in Figs. 6 to 13 definitely confirm the capability of the

target discrimination provided by the method based on the concept of the E-pulses

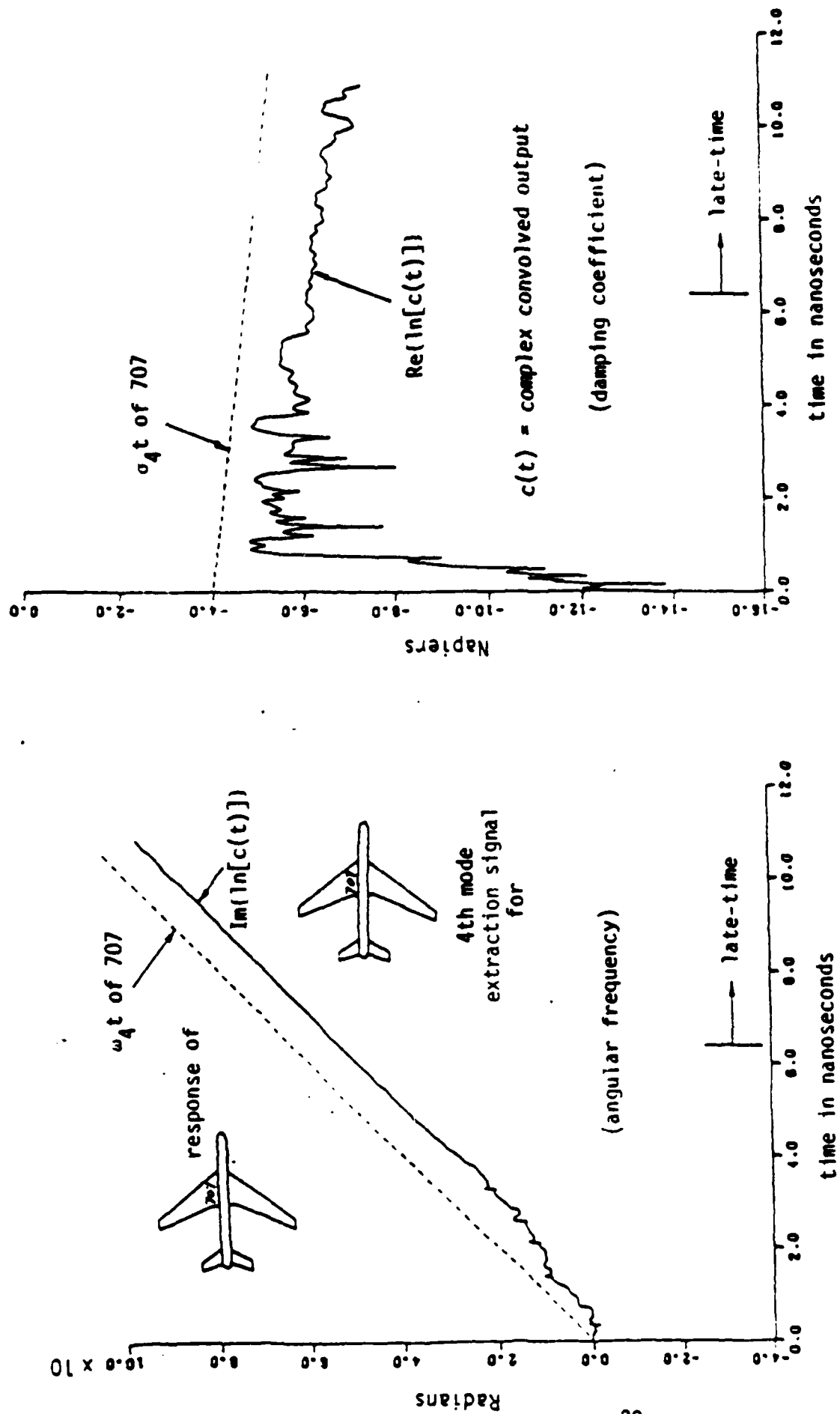and single-mode extraction signals.

Fig. 11. Angular frequency and damping coefficient extracted from the complex convolved output of the fourth mode extraction signal for the 707 target and the 707 measured response.

20

Fig. 12. Angular frequency and damping coefficient extracted from the complex convolved output of the first mode extraction signal for the 707 target and the F-18 measured response.

Fig. 13. Angular frequency and damping coefficient extracted from the complex convolved output of the fourth mode extraction signal for the 707 target and the F-18 measured response.
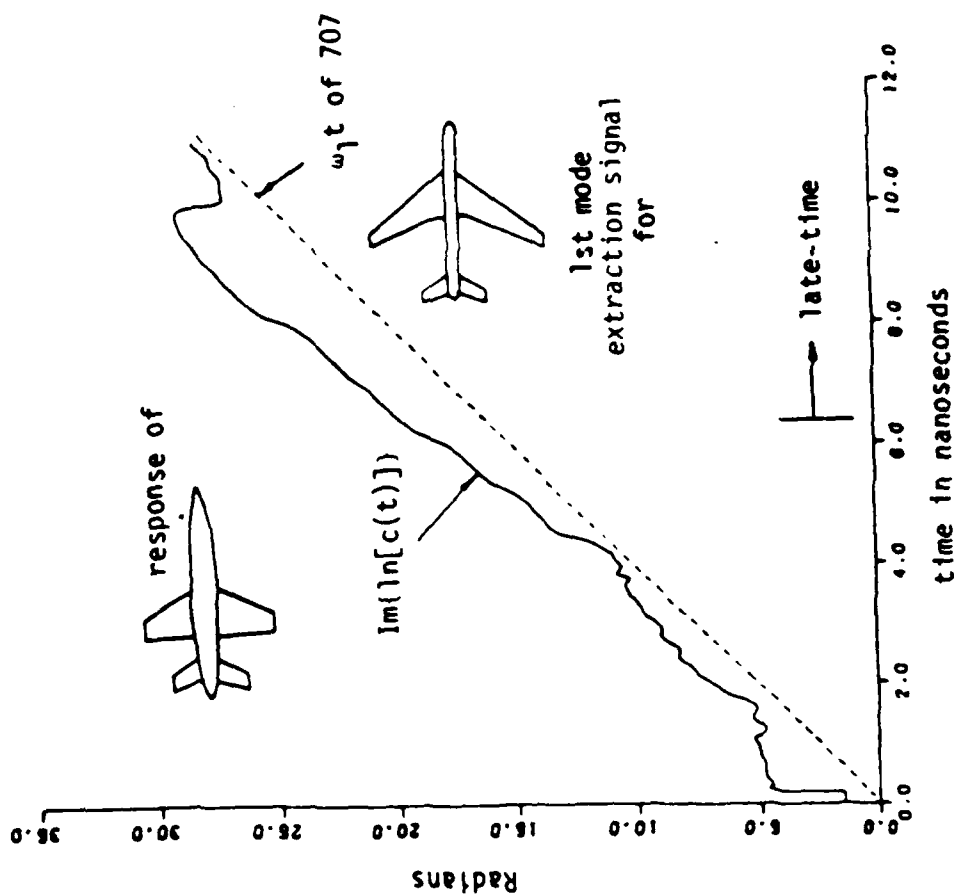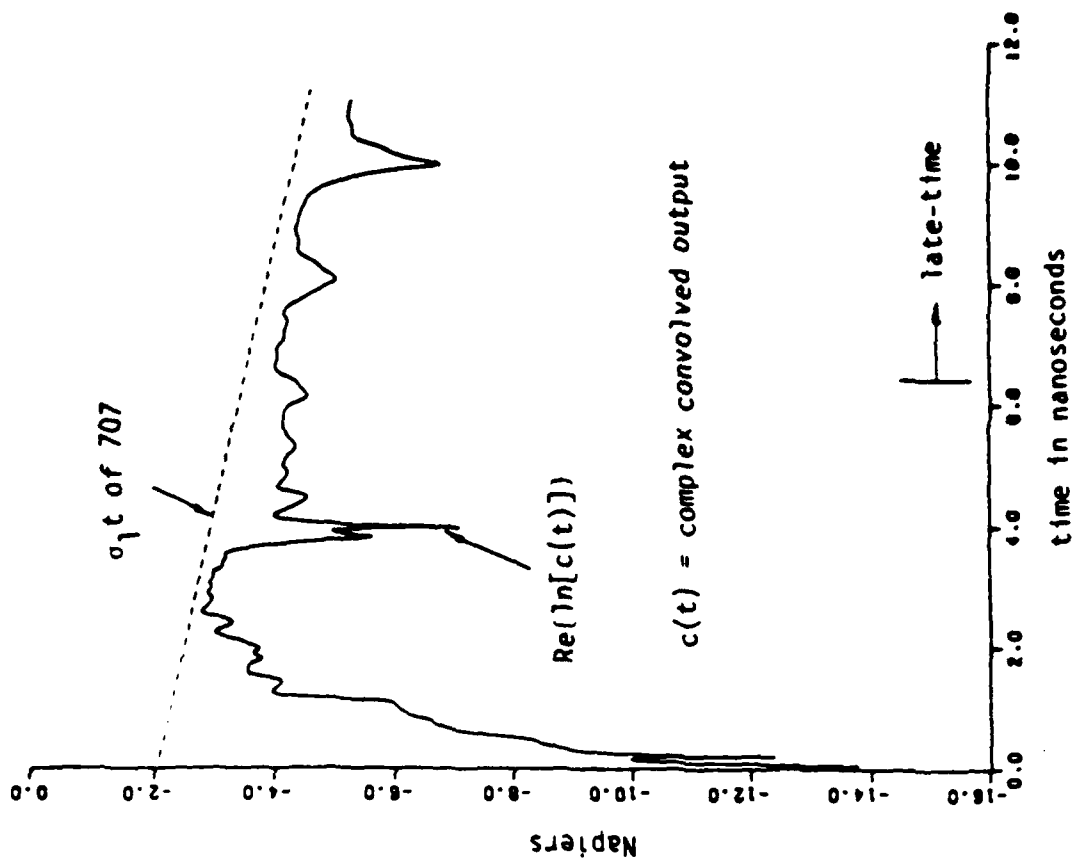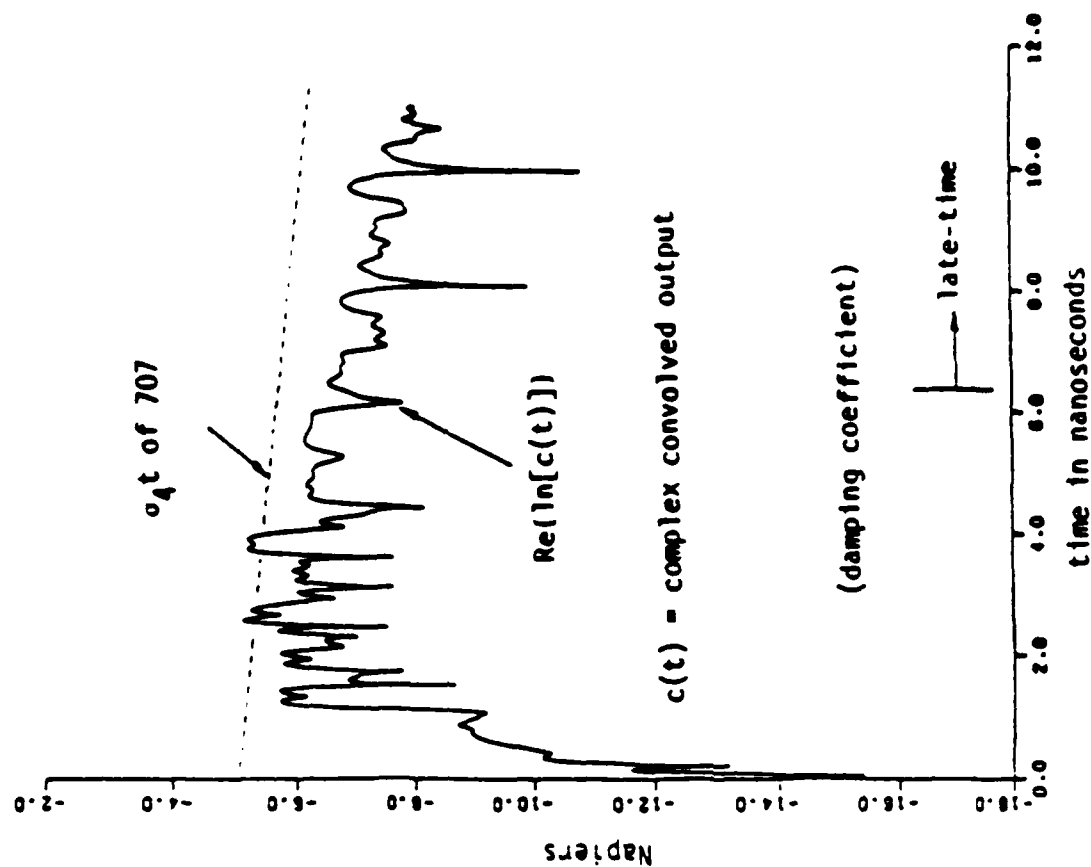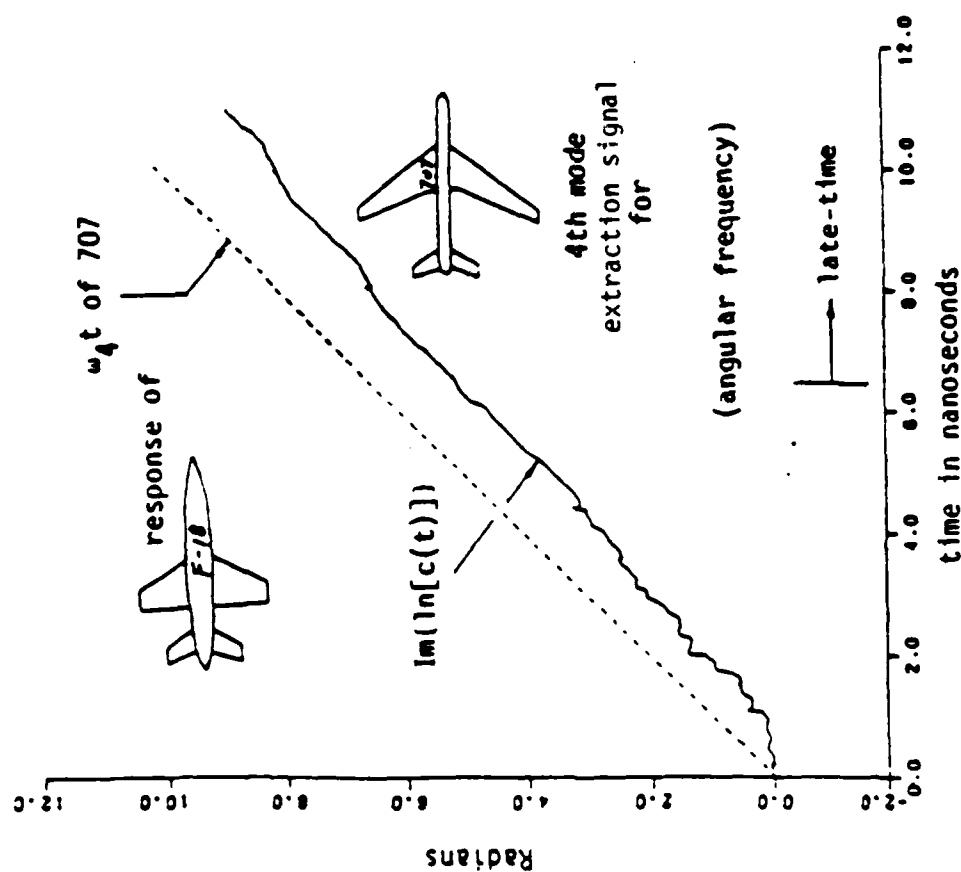
22

It is important to demonstrate that the E-pulse and single-mode extraction signals of a target are aspect-independent. The following examples are given for this purpose.

Fig. 14 shows the convolved outputs of the E-pulse of F-18 model with the pulse responses of F-18 model measured at (a) 0^0 aspect angle, (b) 30^0 aspect angle, (c) 45^0 aspect angle and (d) 60^0 aspect angle. In each case the convolved output gives an insignificant response in the late-time periods. This implies that natural modes of the target were extinguished by its E-pulses and the pulse responses used in the convolution belonged to the F-18 model.

Figure 15 shows the convolved outputs of the E-pulse of F-18 model with the pulse responses of B707 model measured at (a) 0^0 aspect angle, (b) 30^0 aspect angle, (c) 90^0 aspect angle and (d) 180^0 aspect angle. It is observed that the convolved outputs give large late-time responses in all four aspect angles. This indicate that the F-18 E-pulse was convolved with the pulse response of a different target.

Figure 16 shows the convolved outputs of the E-pulse of B707 model with the pulse responses of B707 model measured at (a) 0^0 aspect angle, (b) 30^0 aspect angle, (c) 90^0 aspect angle and (d) 180^0 aspect angle. It is observed that the convolved outputs give small late-time responses in all four aspect angles as expected. This implies that B707 E-pulse was convolved with the pulse responses of the same target.

Figure 17 shows the convolved outputs of B707 E-pulse with the pulse responses of F-18 model measured at (a) 0^0 aspect angle, (b) 45^0 aspect angle, (c) 90^0 aspect angle and (d) 180^0 aspect angle. Large late-time responses are obtained in the convolved outputs for all four aspect angles, signifying that the pulse responses used in the convolution belonged to a target different from B707 model.

23

Fig. 14. Convolved outputs of F-18 E-pulse with pulse responses of F-18 model measured at (a) 0° aspect angle, (b) 30° aspect angle, (c) 45° aspect angle and (d) 60° aspect angle. In each case, a small response was obtained in the late-time period.

24
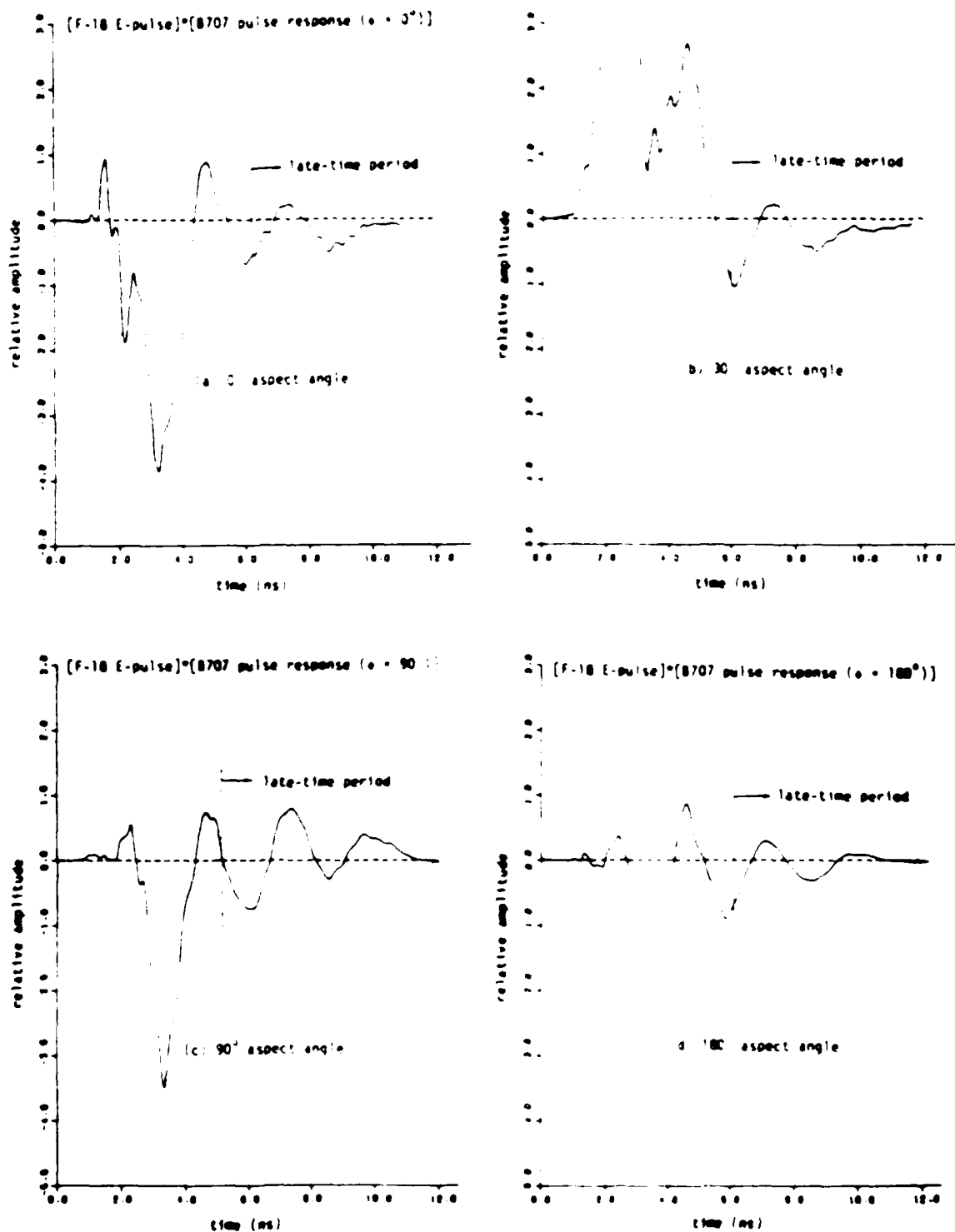
Fig. 15. Convolved outputs of F-18 E-pulse with pulse responses of B707 model
measured at (a) 0° aspect angle, (b) 30° aspect angle, (c) 90°
aspect angle and (d) 180° aspect angle. In each case, a large response
was obtained in the late-time period.

25

Fig. 16. Convolved outputs of B707 E-pulse with pulse responses of B707 model measured at (a) 0° aspect angle, (b) 30° aspect angle, (c) 90° aspect angle and (d) 180° aspect angle. In each case, a small response was obtained in the late-time period.
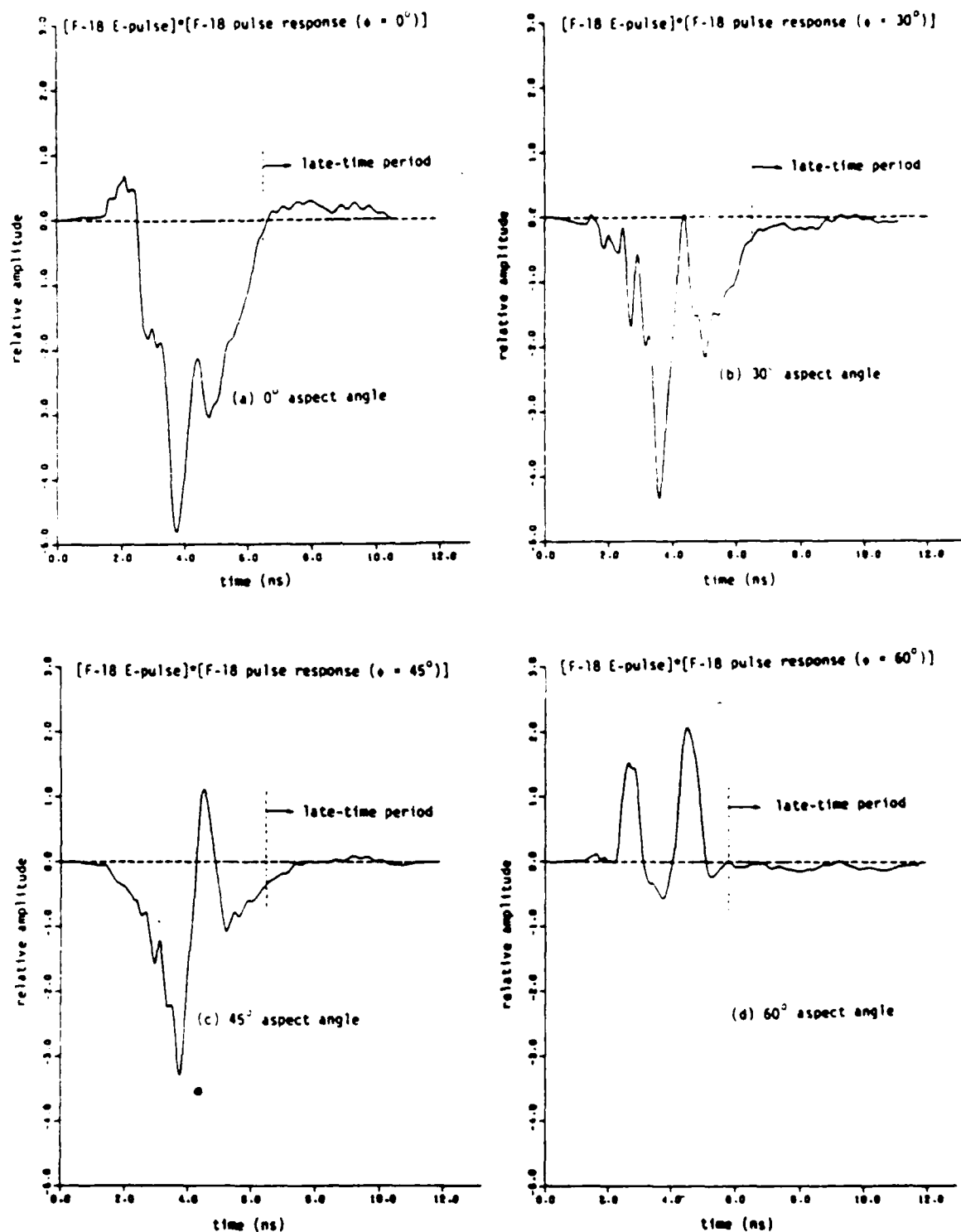
26

Fig. 17. Convolved outputs of B707 E-pulse with pulse responses of F-18 model measured at (a) 0° aspect angle, (b) 45° aspect angle, (c) 90° aspect angle and (d) 180° aspect angle. In each case, a large response was obtained in the late-time period.
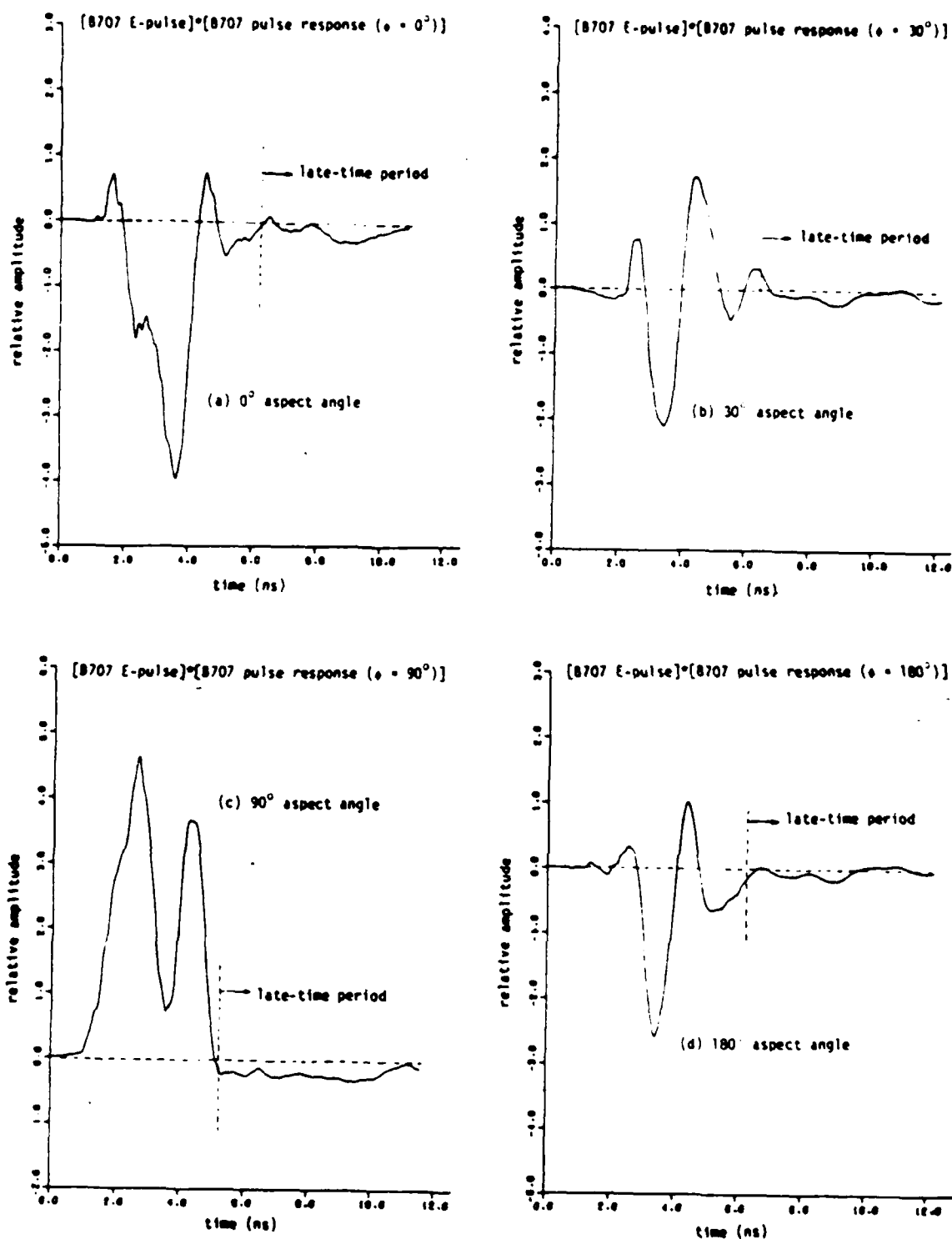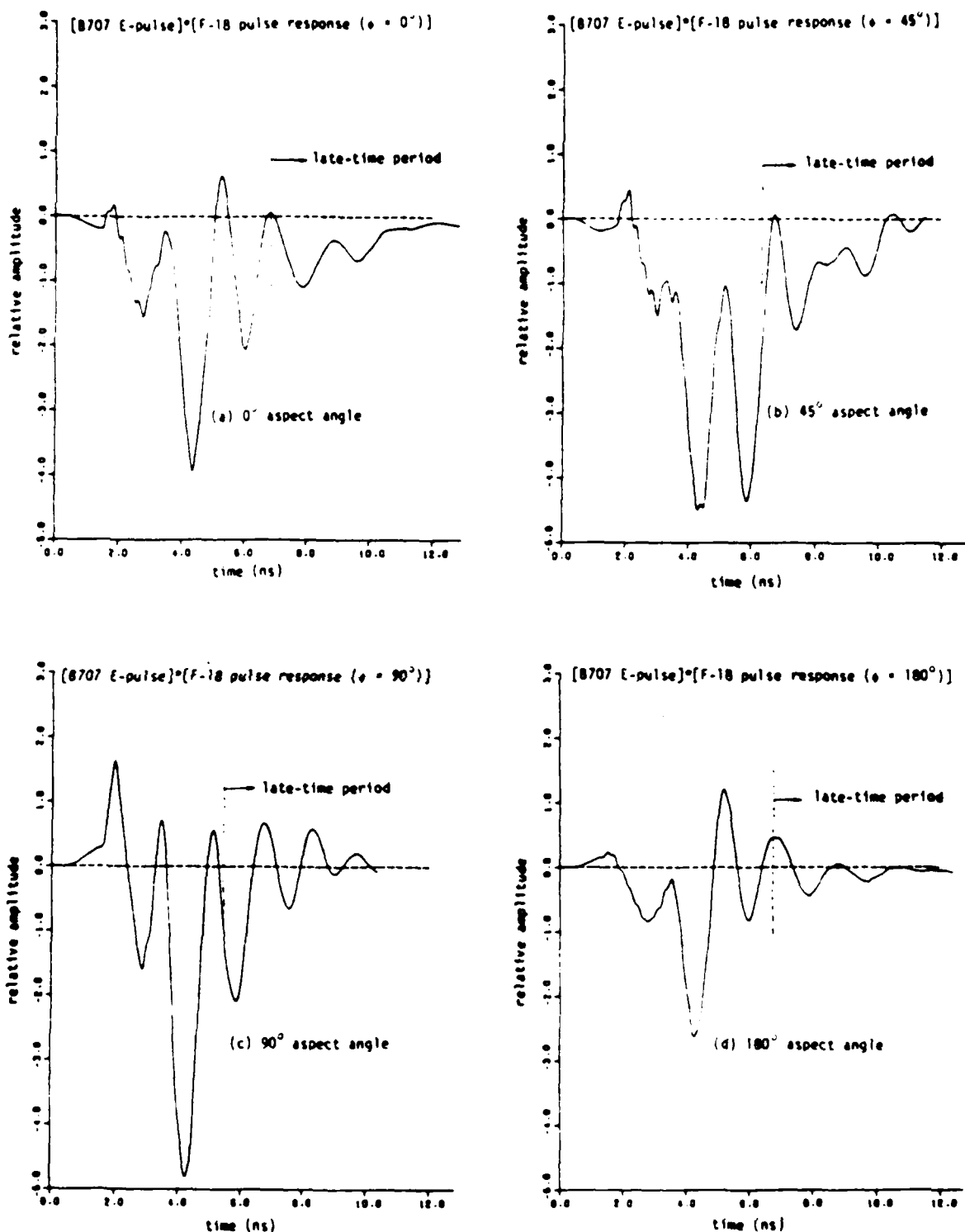
The results of Figs. 14-17 confirm the aspect independency of the E-pulse of a complex target and the feasibility of its use in the target discrimination.

4.   Shaping Extraction Signals by Proper Choice of Basis Functions

In the synthesis of a single-mode extraction signal, it is important for the spectrum of a single-mode extraction waveform to have a large magnitude at the frequency of the mode to be extracted, in comparison to that at the frequencies to be eliminated. This is due to the practical problem of the presence of errors in the measured natural frequencies used to construct the single mode extraction signals. Because of this error, the modes which should be eliminated will actually be extracted. The amplitudes of these modes are, of course, determined by the amount of energy in the extraction signal spectrum at the modal frequencies. Now, if there is a relatively small amount of energy at the frequency to be extracted, these extraneous modes may make a relatively large contribution to the late-time portion of the convolved response, so that the expected target might not be properly identified. This is especially trouble-some for the case of higher mode extraction, where the smaller damping coefficients of the lower order modes to be eliminated allow them to dominate the expected higher order mode in the latter part of the late-time region.

Assume that we wish to extract a single mode with frequency $\hat{s} = \hat{\sigma} + j\hat{\omega}$. Consider using the damped sinusoid functions for the basis functions,

$$f_m(t) = e^{\widetilde{\sigma}_n t} \cos(\widetilde{\omega}_m t + \widetilde{\phi}_m) \tag{29}$$

with the transforms

$$F_m(s) = - \frac{e^{j\widetilde{\phi}_m}}{2} e^{(\widetilde{s}_m - s)\frac{T_e}{2}} \left[\frac{\sinh(\widetilde{s}_m - s)\frac{T_e}{2}}{(\widetilde{s}_m - s)} \right] - \frac{e^{-j\widetilde{\phi}_m}}{2} e^{(\widetilde{s}_m^* - s)\frac{T_e}{2}} \left[\frac{\sinh(\widetilde{s}_m^* - s)\frac{T_e}{2}}{(\widetilde{s}_m^* - s)} \right] \tag{30}$$

28

where $\tilde{s}_m = \tilde{\sigma}_m + j\tilde{\omega}_m$. The choice of $\tilde{\sigma}_m$ and $\tilde{\omega}_m$ determines the usefulness of this set of basis functions. Alone, each $F_m(s)$ has a peak along a line $Re(s) = $ constant near $\omega = \tilde{\omega}_m$. Thus, choosing $\tilde{\omega}_m \approx \Omega$ for each m should result in an E-pulse with a spectrum peaked near Ω.

As a simple numerical example, Fig. 18 shows the reconstruction of the measured pulse response of a McDonnel Douglas F-18 aircraft model (see Fig. 2) The three dominant modes are used in the reconstruction: $s_1 = [-0.164 + j3.29] \times 10^9$, $s_2 = [-0.126 + j7.32] \times 10^9$, and $s_3 = [-0.441 + j9.89] \times 10^9$. Added to this reconstructed response is 10 dB of random noise. The noise can be viewed as perturbing the natural frequencies in the response. Figure 19 shows two forced sine/cos waveforms constructed to excite the second mode of the reconstructed response. The first waveform is synthesized using rectangular pulse basis functions with a forcing function chosen to be another rectangular pulse. The second wave form is constructed from damped sinusoid functions with the frequencies and phases given in the figure. Here, the forcing function is chosen as another damped sinusoid.

Figure 20 shows the spectra (magnitude) of the two extraction signals plotted at $Re(s) = \sigma_2$. While the spectrum of the pulse function E-pulse is seen to have its signal energy concentrated near $\omega = 0$, the spectrum of the damped sinusoid based E-pulse has a majority of its signal energy near the frequency to be excited. The result of this energy concentration can be seen in Fig. 21, which shows the convolutions of the two E-pulses with the noiseless reconstructed response. As expected, each results in a single damped sinusoid in the late-time, but the late-time response due to the damped sinusoid based E-pulse is seen to be relatively much larger. More importantly, Fig. 22 shows the result of convolving each E-pulse with the noisy response of Fig. 18. It is easily seen that the late-time convolved response from the damped

29
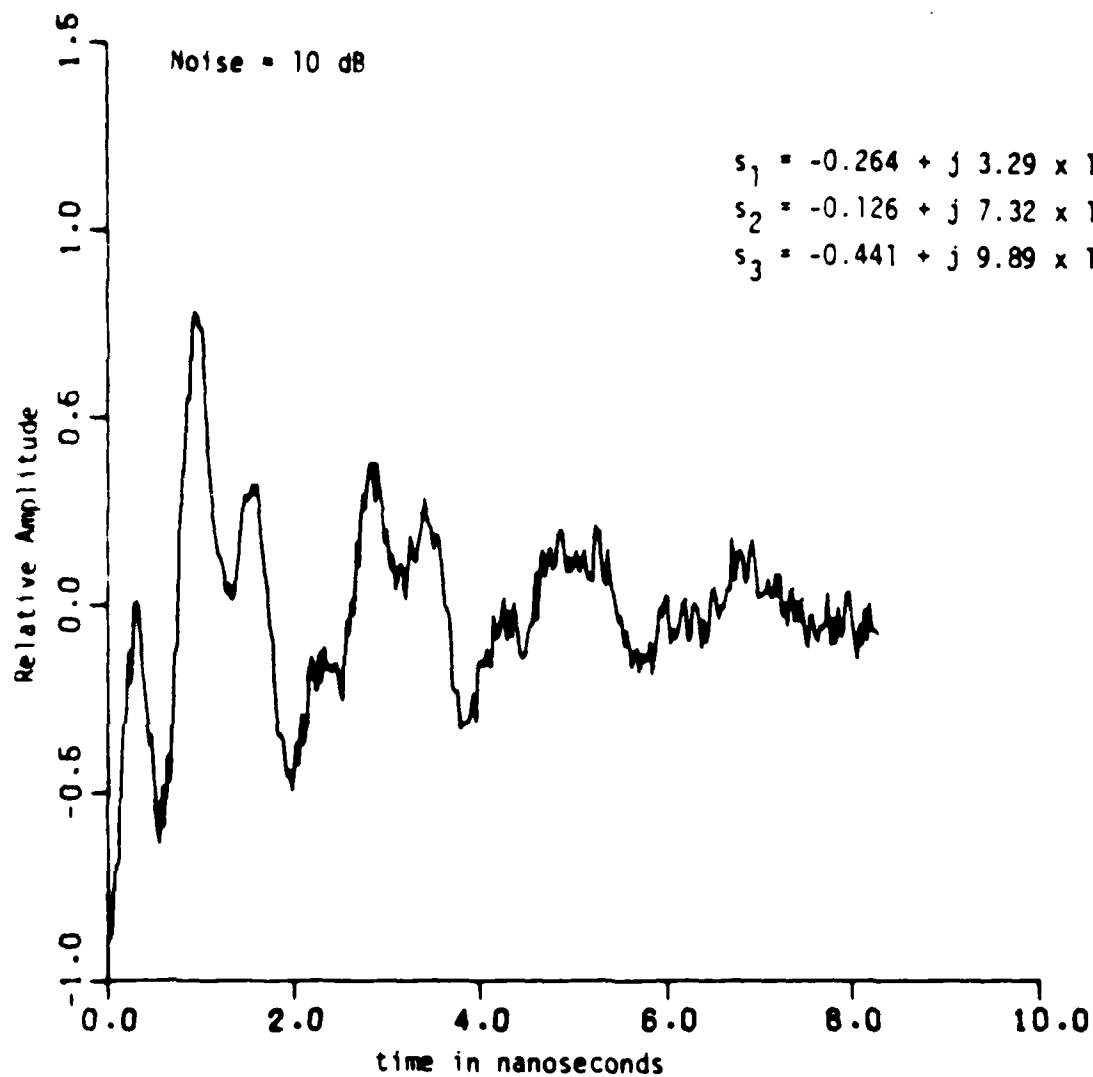
Fig. 18. Reconstruction of measured late-time scattered field response of McDonnel Douglas F-18 aircraft model, using first three natural modes, with 10 dB of random noise added.
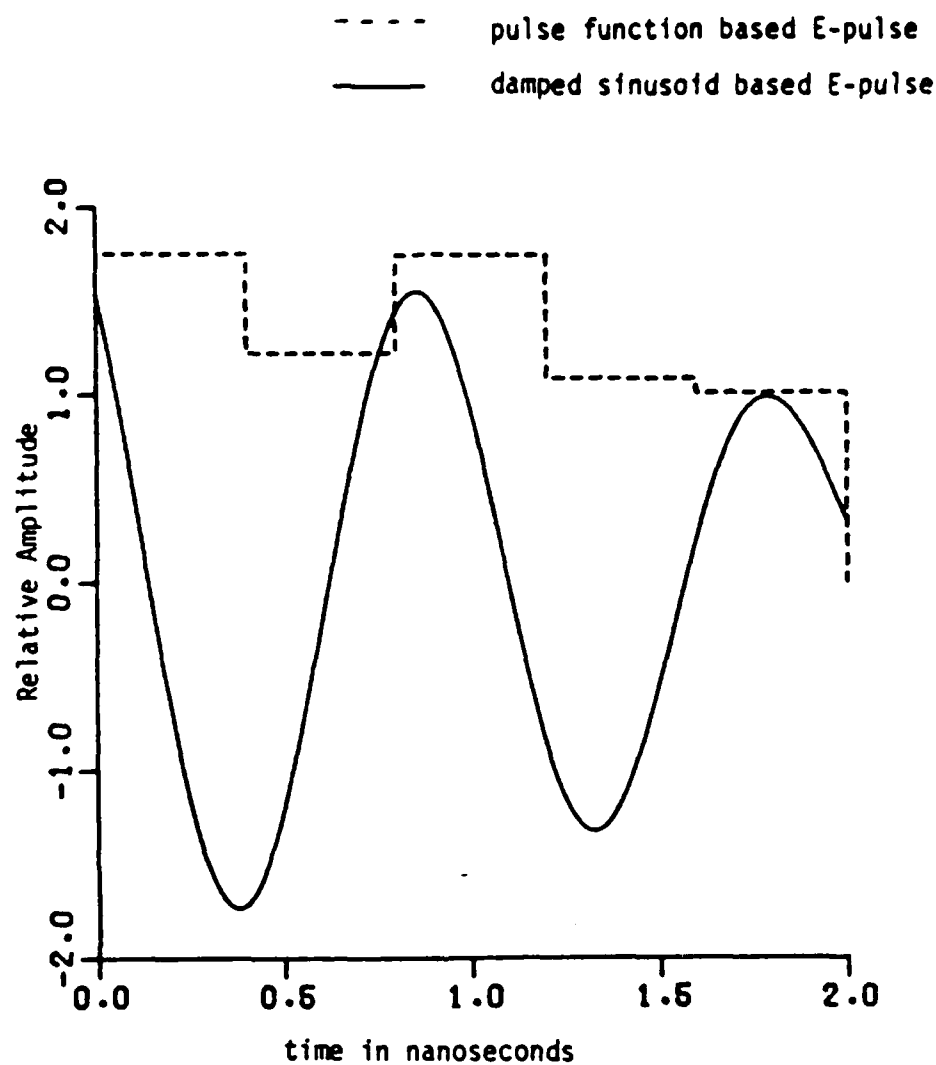
Fig. 19. Pulse function based and damped sinusoid based forced sin/cos single-mode E-pulses synthesized to eliminate first and third modes of reconstructed response, while exciting the second.
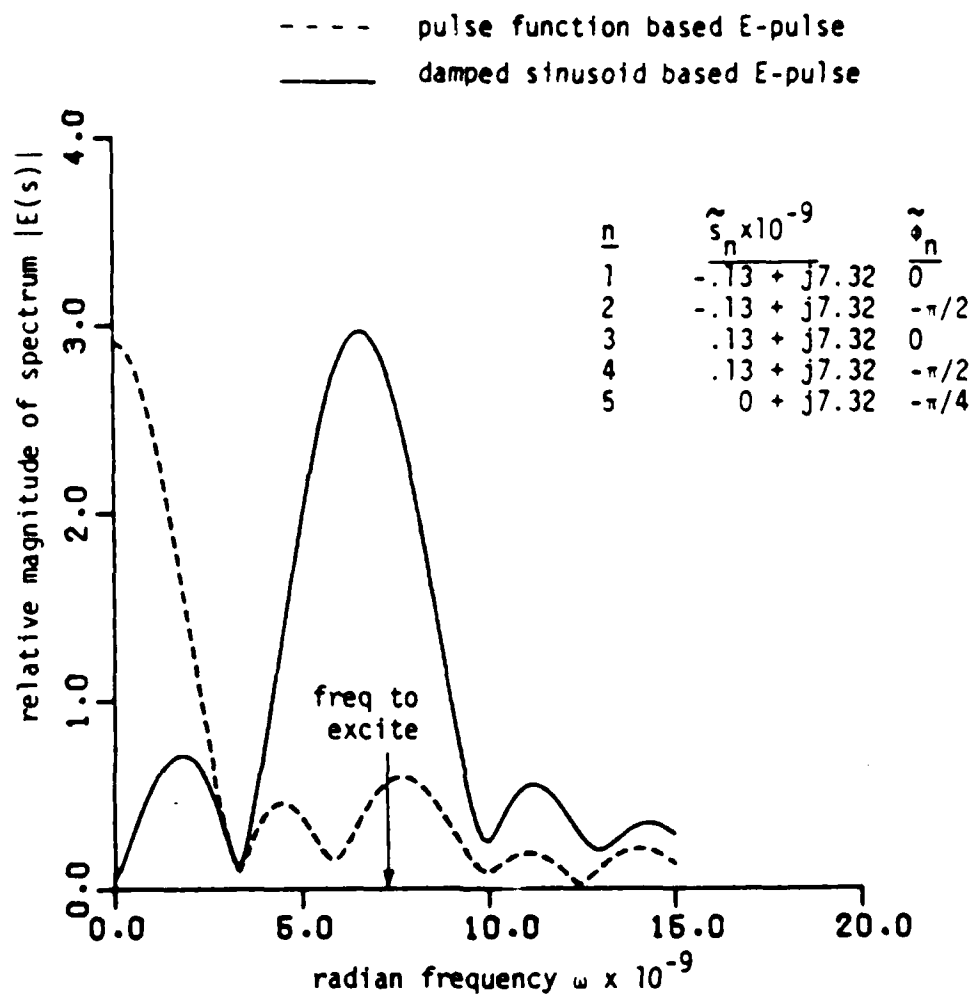
Fig. 20. Spectra of pulse function and damped sinusoid based single-mode E-pulses, plotted at $\sigma = -.13 \times 10^9$. Note peak near $\omega = 7.32 \times 10^9$ for damped sinusoid based E-pulses.
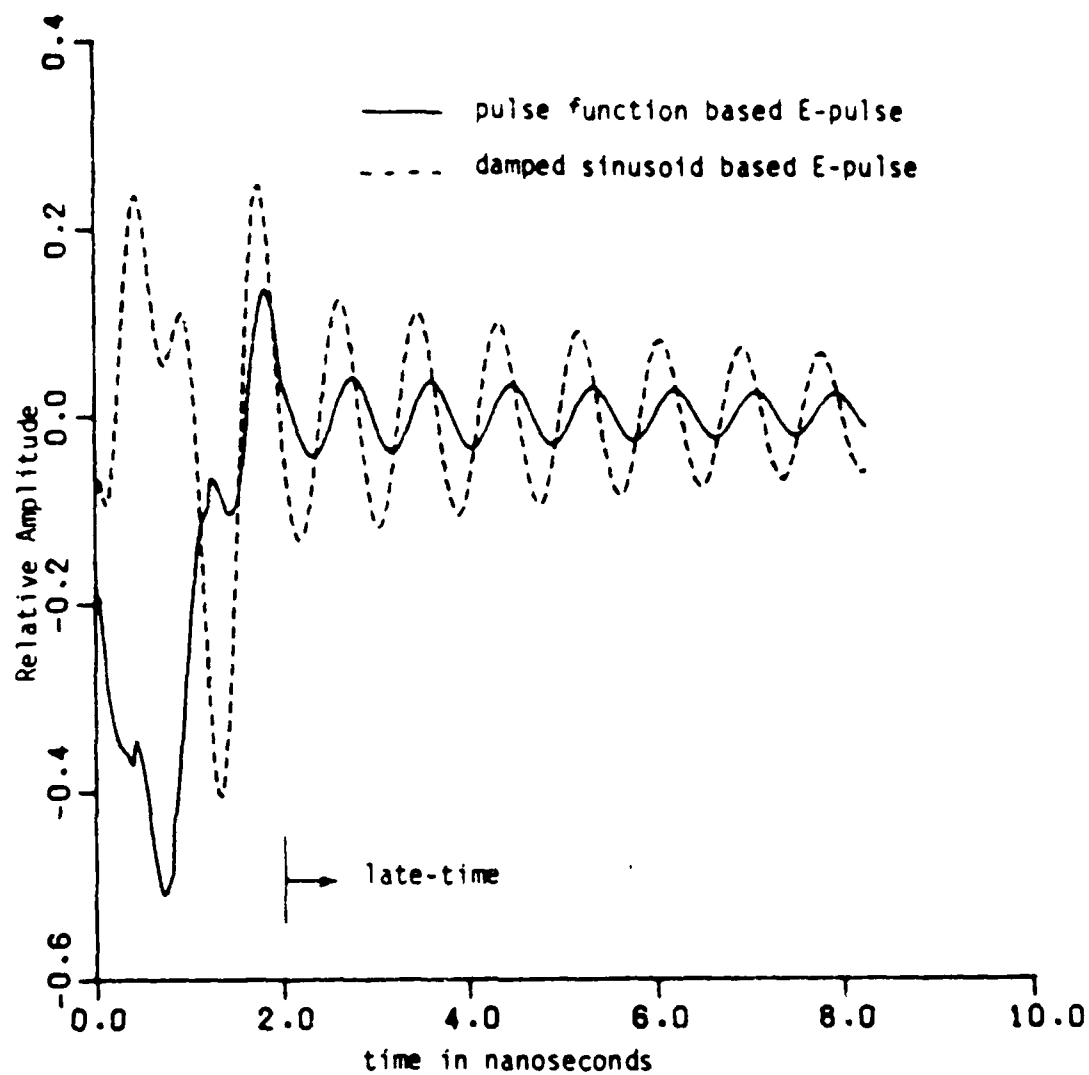
Fig. 21. Convolution of pulse function and damped sinusoid based single-mode E-pulses with noise-free reconstructed response.

Fig. 22. Convolution of pulse function and damped sinusoid based single-mode E-pulses with noisy reconstructed response.

34

sinusoid based E-pulse has been affected much less by the perturbing of the natural frequencies of the reconstructed target response.

There is a need to study the uniqueness of E-pulses and the possiblity of minimizing the duration of the E-pulse. The frequency spectrum of an E-pulse may be controlled by a proper choice of basis functions. Further study on the E-pulse may make it more insensitive to noise. These problems will receive attention in the future.
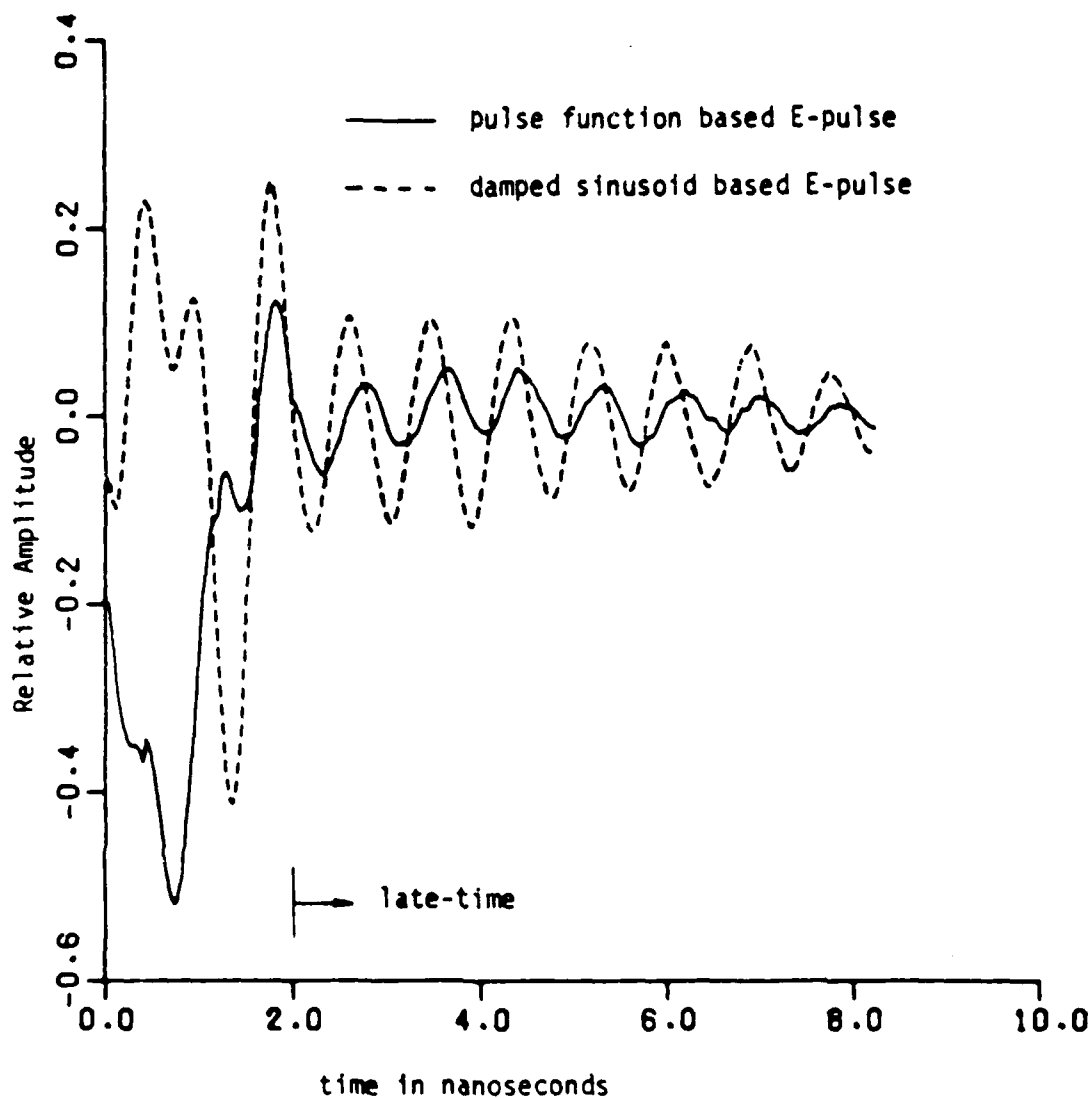
5. New Methods for Extracting the Natural Frequencies of a Complex Target from its Measured Pulse Response

In our scheme, we need to find the natural frequencies of a complex target from its measured pulse response before the E-pulse and single-mode extraction signals of the target can be synthesized. Since the classical Prony's method is known to be extremely sensitive to noise, it is important to develop other methods for this purpose. The first technique developed by us is the Continuation Method which has been published [7] (see Appendix 2) and is being used. This method is not optimal yet and we plan to develop other different methods. Some preliminary results on our three new methods are given below.

The measured scattered field or surface current response, $r(t)$ of a target to a transient pulse waveform is assumed to be composed of a finite number of natural oscillation modes in the late-time period, $t > T_\ell$. The following three techniques attempt to extract the natural frequencies from the sampled representation of $r(t)$.

A. E-Pulse Method

The convolution of an excitation signal with the measured response can be written as

$$q(t) = e(t) * r(t) \tag{31}$$

The natural frequencies contained in $r(t)$ can be extracted by constructing $e(t)$ as an E-pulse. Then, if $r(t)$ is indeed a sum of natural modes, $q(t)$ will be identically zero in the late-time of the convolved response, $t > T_E$. To the extent that $r(t)$ will be contaminated by various types of noise, an estimate of the natural frequencies can be obtained by minimizing the norm of the late-time convolved response

$$\| q(t) \|^2 = \sum_{i=1}^{m} [q(t_i)]^2 \tag{32}$$

with respect to the parameters $\sigma_1, \ldots, \omega_N$ used to construct the E-pulse waveform, where M discrete points are chosen at which to evaluate the norm. The natural frequencies contained in $r(t)$ are taken to be $\sigma_1, \ldots, \omega_N$ at the minimum point.

The benefit of the E-pulse method over the continuation method is that no initial guesses are needed for the phases and amplitudes of the modes, since they are not involved in constructing an E-pulse. This also means that the number of parameters involved in the minimization is reduced by 1/2.

B. Discrete Late-time Minimization

Rather than performing a minimization with respect to the complex frequencies used to construct $e(t)$, this method performs the minimization of (32) with respect to the amplitudes of the basis functions comprising $e(t)$. Extraction of the natural frequencies in $r(t)$ then becomes a two step process. The minimization first provides an estimate of the E-pulse waveform, and then it becomes necessary to determine the complex frequencies that the E-pulse eliminates. This is accomplished by locating the zeroes of the E-pulse spectrum.

If a rectangular pulse function basis set is used to construct the E-pulse, the location of the zeroes of the spectrum is quite simple. The spectrum of the E-pulse becomes

$$E(s) = \mathcal{L}\{e(t)\} = F_1(s)e^{s\Delta} \sum_{n=1}^{N} \alpha_n e^{-sn\Delta} \qquad (33)$$

where $F_1(s)$ is the Laplace transform of the first pulse function, Δ is the pulse width, and α_n is the amplitude of the n'th pulse basis function. Setting (33) equal to zero gives

$$\sum_{n=1}^{N} \alpha_n e^{-sn\Delta} = 0 \qquad (34)$$

which is just a polynomial equation, the roots of which give the complex frequencies eliminated by the E-pulse. These are then taken as an estimate of the natural frequencies contained in $r(t)$.

The benefit of this method over the continuation method is the same as that of the E-pulse method -- half the number of parameters are involved in the minimization, and there is no need for initial guesses of modal amplitude and phase. An initial guess for the basis function amplitudes is provided by choosing initial guesses for the natural frequencies and constructing an E-pulse from them. However, this is the only time at which an E-pulse needs to be constructed, which should represent a considerable savings in execution time over the E-pulse method.

C. Moment Method Approach

This technique is also a two step process, first sovling for an E-pulse using the method of moments to solve the integral equation created by setting the late-time convolved response to zero, and then extracting the frequencies from the E-pulse.

Writing the convolved response (31) in integral form, and assuming that $e(t)$ is an E-pulse results in

$$q(t) = \int_0^{T_e} e(t')r(t - t')dt' = 0 \qquad t > T_E \qquad (35)$$

where T_e is the E-pulse duration. The waveform which solves this integral equation can be calculated by using the moment method. First expand e(t) in a set of basis functions

$$e(t) = \sum_{\ell=1}^{L} \alpha_\ell \, f_\ell(t) \qquad (36)$$

Then rather than forcing (35) to be satisfied at all time $t > T_E$, it is multiplied by a set of M weighting functions $W_m(t)$ and the moments are taken

$$\left\langle W_m(t), \sum_{\ell=1}^{L} \alpha_\ell \int_0^{T_e} f_\ell(t')r(t - t')dt' \right\rangle = 0 \qquad m = 1,2,\ldots,M \qquad (37)$$

where the angle bracket represents the usual inner product.

The integral equation has now been reduced to a homogeneous matrix equation, where M is chosen to be equal to the number of basis functions used to construct e(t). A solution to this equation demands that the determinant of the coefficient matrix be zero. This results in discrete solutions for the E-pulse duration T_e. Although a search is required for these durations, the amount of complexity involved is much less than that of either the E-pulse method or the direct late-time minimization method, since now only one parameter is involved.

Once the E-pulse waveform is determined, the complex frequencies eliminated by the E-pulse are taken as estimates of the natural frequencies in r(t). If e(t) is constructed using pulse basis functions, then the detrmination of these complex frequencies proceeds exactly as in the direct late-time minimization method, by the solution to a polynomial equation.

Two choices of weighting function $W_m(t)$ used in (37) have been investiated. Using delta functions is equivalent to point matching, and requires that equation (35) hold at discrete points in the late-time. Using rectangular pulse functions requires that an average value of the late-time convolved

response be zero, and should provide improved results if r(t) is contaminated by random noise.

The benefit of the moment method approach over the continuation method is that no minimization is required. It is only necessary to repeatedly solve a system of linear equations, which should be much less time consuming.

It is important to prove the reliability of each of these methods under two important conditions: in the presence of random noise, and with the number of modes present underestimated. If the routines work well when the number of modes is underestimated, it is possible to begin by assuming very few modes, and then slowly increasing the number while using the previous results as initial guesses.

To test the performance of the methods, assume an r(t) composed of three modes plus a DC level

$$r(t) = 0.1 + 1\ e^{-0.2601t}\cos(2.906t + 1) + 0.5\ e^{-0.3808t}\cos(6.007t + 2)$$
$$+ 0.3\ e^{-0.4684t}\cos(9.060t + 3) \tag{38}$$

The natural frequencies used in constructing r(t) are just the first three of the thin cylinder target, and the amplitudes have been chosen to accentuate the lower frequency modes. This response is then sampled at 500 equally spaced points between t = 0 and t = 10. Tables 1 and 2 show the results of using the described methods in the presence of various amounts of random noise and with the number of modes present underestimated. Shown for comparison are the results from using the continuation method and straight-forward Prony's method. Here noise has been created by perturbing each sampled point in the response by a random amount not exceeding a certain percentage of the maximum 'absolute' value of the response. Since the results for the direct late-time minimization method and the E-pulse method are nearly identical, those for the E-pulse technique have been omitted from the tables for brevity

Noise	Natural frequencies	Exact Values	PM	LTM	MMPF	MMDF	CM
5%	σ_1 ω_1	-0.2601 2.906	-0.4593 2.783	-0.2614 2.909	-0.2584 2.903	-0.2697 2.936	-0.2575 2.899
	σ_2 ω_2	-0.3808 6.007	0.0179 3.491	-0.3976 6.005	-0.4294 6.032	-0.3847 6.031	-0.3964 6.056
	σ_3 ω_3	-0.4684 9.060	-0.3043 0.7620	-0.5229 8.959	-0.0414 8.961	-0.2284 8.924	-0.4717 9.149
10%	σ_1 ω_1	-0.2601 2.906	-0.3533 2.694	-0.2729 2.912	-0.2537 2.899	-0.2781 2.957	-0.2538 2.892
	σ_2 ω_2	-0.3808 6.007	0.1410 2.981	-0.3910 5.955	-0.4788 6.075	-0.3838 6.022	-0.4099 6.112
	σ_3 ω_3	-0.4684 9.060	-0.1717 0.6729	-0.4708 8.973	0.0332 9.221	-0.0878 8.907	-0.4845 9.225
25%	σ_1 ω_1	-0.2601 2.906	-0.3917 2.775	-0.2574 2.933	-0.2419 2.882	-0.2961 3.009	-0.2343 2.862
	σ_2 ω_2	-0.3808 6.007	0.0614 2.117	-0.3393 5.996	-0.4999 6.208	-0.4344 5.946	-0.4036 6.322
	σ_3 ω_3	-0.4684 9.060	0.2330 0.8231	1.272 8.541	0.3077 9.312	0.0990 8.899	-0.5936 9.527

PM: Prony's method, LTM: Direct late-time minimization
MMPF: Moment method-pulse function weighting
MMDF: Moment method-delta function weighting
CM: Continuation Method

Table 1. Performance of various natural frequency extraction schemes in the presence of random noise.

No. of modes expected	Natural frequencies	Exact values	PM	LTM	MMPF	MMDF	CM
1	σ_1 ω_1	-0.2601 2.906	-0.0468 0.4251	-0.2589 2.897	-0.2460 2.909	-0.2606 2.896	-0.2171 2.848
2	σ_1 ω_1	-0.2601 2.906	-0.3649 1.883	-0.2603 2.907	-0.2598 2.905	-0.2977 2.914	-0.2486 2.889
	σ_2 ω_2	-0.3808 6.007	-0.6549 0.8467	-0.3803 6.009	-0.3312 6.007	-0.3781 6.056	-0.3523 5.882

Key: See Table 1

Table 2. Performance of various natural frequency extraction schemes when the number of modes present in the response is underestimated.

It is obvious that each new method performs quite will both in the presence of random noise and when the number of modes present is underestimated. As expected, Prony's method fails under both circumstances.

We will apply these three new methods to the measured pulse responses of various complex targets in the future. If any of these new methods is proved to be more accurate than the Continuation Method, it will be accepted as our new tool for synthesizing the E-pulses of complex targets.

6. Future Plans

The following topics will receive major attention in the future.

(1) Synthesis of E-pulses and single-mode extraction signals for various complex targets, including various types of aircrafts and scale vehicles, from the measured pulse responses of their scale model.

We will apply our developed technique for synthesizing the E-pulses and single-mode extraction signals to various complex targets to establish its versatility and accuracy. The complexity of experimental scale models of aircrafts will be increased by adding fine structures to the models. When this happens, the number of natural frequencies of the model will be increased, and consequently, the synthesis of the discriminant signals will become more difficult. We will test whether our technique can handle this problem.

(2) Refinement of the technique based on frequency-domain analysis.

In the synthesis of a single-mode extraction signal for a target the signal waveform and its frequency spectrum are found to be dependent on the choice of basis functions. From the frequency domain viewpoint, it is possible to select appropriate basis functions which may lead to an effective extraction (with a maximum power) of the desired natural mode, and at the same time, eliminating all other natural modes. We plan to improve the quality of the single-mode extraction signal using this concept. This is the continuation of the study described in Section 4.

(3) Improvement and modification of experimental systems.

The short term plan for the improvement of our experimental system is to add a new sampling scope, a Tektronix 7854 digital waveform processing oscilloscope (DWPO), and the modification of associated instrumentation. The long term plan for our experimental system is to set up a free-space scattering range inside an anechoic chamber. A ground plane will not be used

43

but new transmitting and receiving antennas need to be purchased. Some other components of the system may need to be altered. To accomplish this long term plan, extra funding may be needed in the future.

4. Measurement of target natural frequencies using current and charge probes located on the target surface.

We have measured the induced current on a wire target excited by a Gaussian pulse with a current probe. From the late-time part of the induced transient current it was possible to extract several of the target's natural frequencies. The attempt to measure the induced transient charge on the surface of a complex target with a charge probe was not very successful. We plan to pursue this topic in the future.

5. New methods for extracting the natural frequencies of a complex target from its measured pulse response.

We will continue to develop new methods for extracting the natural frequencies of a complex target from its measured pulse response. The new methods will include the "second generation" continuation method, the E-pulse method, the discrete late-time minimization method, and the moment method as described in Section 5. We will compare the performance of each method and finally select the optimal one for our application.

(6) New topics relating to radar target detection.

One of the important new topics which may have great value in radar target detection is the utilization of the early-time response of the radar return. The early-time response contains much more energy than the late-time response does. However, the former does not contain aspect-independent parameters like the latter does. Therefore, it may be extremely difficult to develop an aspect-independent scheme using the early-time response of the target. We may consider this problem in the future as a long term project.

44

Personnel

The following personnel have participated in this research program.

1. Kun-Mu Chen, Professor and Principal Investigator

2. Dennis P. Nyquist, Professor and Senior Investigator

3. Byron Drachman, Professor and Senior Investigator

4. Edward Rothwell, Graduate Assistant

5. Wei-Min Sun, Graduate Assistant

6. Neila Gharsallah, Graduate Assistant

Publication

The following papers have been published in technical journals or presented
in the International or National meetings over the past year.

1. Edward Rothwell, D.P. Nyquist, and K.M. Chen, "Synthesis of Kill-pulse to excite selected target modes," presented at 1984 International IEEE/AP-S Symposium, Boston, June 25-29, 1984.

2. Lance Webb, and K.M. Chen, "Target discrimination using K-pulse, single-mode excitation signals and Prony's method," presented at 1984 International IEEE/AP-S Symposium, Boston, June 25-29, 1984.

3. Byron Drachman, "Continuation methods for identification of the natural frequencies of an object using a measured response, and the deconvolution problem revisited," presented at 1984 International IEEE/AP-S Symposium, Boston, June 25-29, 1984.

4. Edward Rothwell, and Byron Drachman, "Use of a continuation method for the extraction of natural frequencies from a target response: Experimental and numerical results," presented at 1984 National Radio Science Meeting, Boston, June 25-29, 1984.

5. Byron Drachman and E. Rothwell, "A continuation method for identification of the natural frequencies of an object using a measured response," IEEE Trans. on Antennas and propagation, AP-33, No. 4, April 1985, pp. 445-450.

6. Edward Rothwell, K.M. Chen, D.P. Nyquist, N. Gharsallah and B. Drachman, "Frequency domain E-pulse synthesis and target discrimination," presented at 1985 International IEEE/AP-S Symposium, Vancouver, Canada, June 17-21, 1985.

7. Edward Rothwell, D.P. Nyquist, K.M. Chen and B. Drachman, "Radar target discrimination using Extinction-pulse technique," IEEE Trans. on Antennas and Propagation, AP-33, No. 9, Sept. 1985, pp. 929-937.

References

[1] I. Gerst and J. Diamond, "The elimination of intersymbol interference by input signal shaping," Proceeding of the IRE, July 1961, pp. 1195-1203.

[2] E.M. Kennaugh, "The K-pulse concept," IEEE Trans. on Antennas and Propagation, AP-20, No. 2, March 1981, pp. 327-331.

[3] E. Rothwell, D.P. Nyquist, K.M. Chen and B. Drachman, "Radar target discrimination using the extinction-pulse technique," IEEE Trans. on Antennas and Propagation, AP-33, No. 9, Sept. 1985, pp. 929-937.

[4] E. Rothwell, K.M. Chen, D.P. Nyquist, N. Gharsallah and B. Drachman, "Frequency-domain E-pulse synthesis and target discrimination," 1985 International IEEE/AP-S Symposium, Vancouver, Canada, June 17-21, 1985, Symposium Digest, pp. 285-288.

[5] E. Rothwell, K.M. Chen, D.P. Nyquist and B. Drachman, "Synthesis of kill-pulse to excite selected target modes," 1984 International IEEE/AP-S Symposium, Boston, June 25-29, 1984, Symposium Digest, pp. 15-18.

[6] K.M. Chen, "Radar waveform synthesis for target identification," Final Report for Naval Air Systems Commands, Division of Engineering Research, Michigan State University, East Lansing, Michigan, 1984.

[7] B. Drachman and E. Rothwell, "A continuation method for identification of the natural frequencies of an object using a measured response," IEEE Trans. on Antennas and Propagation, AP-33, No. 4, April 1985, pp. 445-450.

Radar Target Discrimination Using the Extinction-Pulse Technique

EDWARD ROTHWELL, STUDENT MEMBER, IEEE, D. P. NYQUIST, MEMBER, IEEE, KUN-MU CHEN, FELLOW, IEEE, AND BYRON DRACHMAN

Abstract—An aspect independent radar target discrimination scheme based on the natural frequencies of the target is considered. An extinction-pulse waveform upon excitation of a particular conducting target results in the elimination of specified natural modal content of the scattered field. Excitation of a dissimilar target produces a noticeably different late-time response. Construction of appropriate extinction-pulse waveforms is discussed, as well as the effects of random noise on their application to thin cylinder targets. Also presented is experimental verification of this discrimination concept using simplified aircraft models.

I. INTRODUCTION

RADAR TARGET identification methods using the time-domain response of a target to a transient incident waveform have generated considerable interest recently [1]-[4]. One of the most intriguing schemes involves the so-called "kill-pulse" technique as first described by Kennaugh [5]. A Kill-pulse (K-pulse) is an excitation waveform synthesized in such a way as to minimize a transient scattered field response. Target discrimination results from the unique correspondence of a K-pulse to a particular target; excitation of a dissimilar target yields a "larger" response.

This paper describes a related "extinction-pulse" (E-pulse) concept, based on the natural resonance of a conducting radar target via the singularity expansion method (SEM) [6]. The time domain electric field scattered by the target is divided into an early-time, forced response period when the excitation waveform is traversing the target, and a late-time, free oscillation period that exists after the excitation waveform has passed [7], [8]. The early-time response is not utilized due to its complicated nature. The late-time response can be decomposed into a sum of damped sinusoids oscillating at frequencies determined entirely by the geometry of the target. An E-pulse is then viewed as a transient, finite duration waveform which annihilates the contribution of a select number of these natural resonances to the late-time response. A related target identification scheme based on natural target resonances has been examined by Chen [9].

Target discrimination using this SEM viewpoint is easily visualized. Each target can be described by a set of natural frequencies. An E-pulse designed to annul certain natural resonances of one target will excite those of a target with

different natural frequencies, resulting in a different scattered field. Also made apparent is the aspect-independent nature of the E-pulse. Since the values of the target resonance frequencies are independent of the excitation waveform, the E-pulse will eliminate the desired natural modal content of the late-time scattered field regardless of the orientation of the target with respect to the transmitting and receiving antennas.

It is important to note that the E-pulse waveform need not be transmitted to employ this concept. It is assumed that an excitation waveform with finite usable bandwidth will be used to excite the target, resulting in a measured scattered field with the desired (finite) modal content. The E-pulse can then be convolved numerically with the measured target response, yielding results analogous to E-pulse transmission. If the maximum modal content of the target scattered field can be estimated from the frequency content of the excitation pulse, then the E-pulse waveform can be constructed to yield a null late-time convolved response.

After an initial presentation of the SEM representation of the backscattered field excited by a transient incident wave and calculation of the corresponding impulse response, two types of E-pulses, forced and natural, will be discussed. The results are then specialized to a thin cylinder target, which has an impulse response amenable to analytic calculation. Target discrimination using the natural thin cyclinder E-pulse, as well as the effects of random noise are also investigated. Lastly, experimental verification of the E-pulse concept is presented.

II. BACKSCATTERED FIELD EXCITED BY TRANSIENT INCIDENT WAVE

A perfectly conducting radar target is illuminated by a plane electromagnetic wave as shown in Fig. 1. The electric field associated with this transient wave can be written in the Laplace transform domain as

$$\vec{E}^i(\vec{r}, s) = \vec{\zeta}e(s)e^{-s\vec{k}\cdot\vec{r}/c} \tag{1}$$

where $\vec{r}$ is a position vector in a coordinate system local to the target, $\vec{\zeta}$ is a constant vector specifying the polarization of the wave, $\vec{k}$ is a unit vector in the direction of propagation, and $e(t)$ represents the time dependence of the incident field. The current $\vec{k}$ induced on the surface of the target is given by the solution to the transform domain E-field integral equation

$$\int_s \left[\nabla' \cdot \vec{k}(\vec{r}', s)(\vec{i} \cdot \nabla) - \frac{s^2}{c^2}\vec{i} \cdot \vec{k}(\vec{r}', s) \right] \frac{e^{-sR/c}}{4\pi R} ds$$
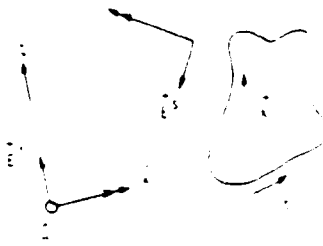
$$= -se_o\vec{i} \cdot \vec{E}^i(\vec{r}, s) \tag{2}$$

Fig 1   Illumination of a conducting target by an incident electromagnetic wave

where $\hat{t}$ is a unit vector tangent to the surface of the target at the point $\vec{r}$ on S, and $R = |\vec{r} - \vec{r}'|$. The surface current can also be expanded using the SEM representation

$$\vec{R}(\vec{r}, s) = \sum_{\alpha=1}^{N} a_\alpha \vec{R}_\alpha(\vec{r})(s - s_\alpha)^{-1} + \vec{W}(\vec{r}, s) \qquad (3)$$

where $\vec{W}(\vec{r}, s)$ represents any entire function contribution to the current, and it is assumed that only a finite number of natural modes are substantially excited by the incident field. It is further assumed that the only singularities of $\vec{R}(\vec{r}, s)$ in the finite complex s-plane are simple poles at natural frequencies $s_\alpha = \sigma_\alpha + j\omega_\alpha$. Then, $\vec{R}_\alpha(\vec{r})$ represents the current distribution of the αth natural mode, and a_α is the "class-1" coupling coefficient given by Baum [10].

The far-zone backscattered electric field can be computed by integrating the current distribution over the surface of the target. The $\hat{\zeta}$ component of backscattered field can then be written as

$$E_\zeta^s(r, s, \hat{k}) = \frac{e^{-sr/c}}{r} e(s) H(s, \hat{k}, \hat{\zeta}) \qquad (4)$$

where $r = |\vec{r}|$ and $H(s, \hat{k}, \hat{\zeta})$ is the aspect dependent transfer function of the target. Using (3) to represent the surface current, the transfer function can be inverse transformed to determine the backscatter impulse response of the target.

Because of the entire function contribution to the current, the impulse response will exhibit two distinct regions. The early-time, forced component represents the backscattered field excited by currents during the time when the impulse is traversing the target. it has a duration equal to twice the one-way maximal transit time of the target T. The late-time free oscillation component is composed purely of a sum of constant amplitude natural modes and exists for all time $t > 2T$ as

$$h(t, \hat{k}, \hat{\zeta}) = \sum_{n=1}^{N} a_n(\hat{k}, \hat{\zeta}) e^{\sigma_n t} \cos(\omega_n t + \phi(\hat{k}, \hat{\zeta})), \quad t > 2T \qquad (5)$$

where it has been assumed that the entire function makes no contribution to the late-time component [6]. Thus, the $\hat{\zeta}$ component of the far-zone backscattered field is given simply by the convolution of the time domain incident field and the impulse response, and is also composed of forced and freely oscillating portions.

III. Incident E-Pulse Waveform Synthesis

To synthesize an E-pulse for a particular target, the convolutional representation of the backscattered field is

written in integral form using the impulse response of (5) as

$$E_\zeta^s(t, \hat{k}) = \int_0^{T_e} e(t') h(t - t', \hat{k}, \hat{\zeta}) \, dt'$$

$$= \int_0^{T_e} e(t') \sum_{n=1}^{N} a_n(\hat{k}, \hat{\zeta}) e^{\sigma_n(t - t')} \cos[\omega_n(t - t')$$

$$+ \phi_n(\hat{k}, \hat{\zeta})] \, dt' \qquad (6)$$

This response is valid for the late-time portion of the scattered field. $t > T_L = T_e + 2T$, where T_e is the duration of $e(t)$. The excitation waveform becomes an E-pulse when the scattered field is forced to vanish identically in the late-time. Rewriting (6) and employing this condition yields a defining equation for the E-pulse

$$\sum_{n=1}^{N} a_n(\hat{k}, \hat{\zeta}) e^{\sigma_n t} [A_n(T_e) \cos(\omega_n t + \phi_n(\hat{k}, \hat{\zeta}))$$

$$+ B_n(T_e) \sin(\omega_n t + \phi_n(\hat{k}, \hat{\zeta}))] = 0, \qquad t > T_L = T_e + 2T \qquad (7)$$

where the coefficients $A_n(T_e)$ and $B_n(T_e)$ are given by

$$\left\{ \begin{array}{c} A_n(T_e) \\ B_n(T_e) \end{array} \right\} = \int_0^{T_e} e(t') e^{-\sigma_n t'} \left\{ \begin{array}{c} \cos \omega_n t' \\ \sin \omega_n t' \end{array} \right\} dt' \qquad (8)$$

The linear independence of the damped sinusoids in (7) requires $A_n(T_e) = B_n(T_e) = 0$ for all $1 \le n \le N$.

It is important to note that $A_n(T_e)$ and $B_n(T_e)$ are independent of the aspect parameters $\hat{k}$ and $\hat{\zeta}$, verifying the aspect independence of the E-pulse. This is a direct consequence of the separability of the terms of the impulse response.

A physical interpretation of the E-pulse can be facilitated by decomposing the excitation waveform as shown in Fig 2 as

$$e(t) = e^f(t) + e^e(t) \qquad (9)$$

where $e^f(t)$ is an excitatory component nonvanishing during $0 \le t < T_d$, the response to which is subsequently extinguished by $e^e(t)$ which follows during $T_d \le t \le T_e$. Substituting (9) into (8) and using $A_n(T_e) = B_n(T_e) = 0$ yields
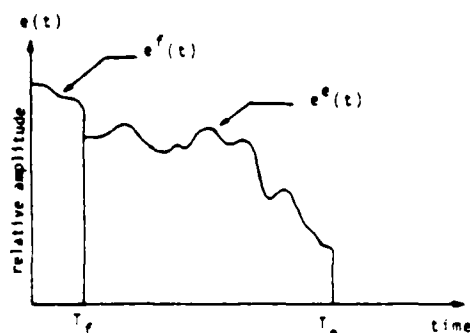
$$\int_{T_d}^{T_e} e^e(t') e^{-\sigma_n t'} \left\{ \begin{array}{c} \cos \omega_n t' \\ \sin \omega_n t' \end{array} \right\} dt'$$

$$= -\int_0^{T_d} e^f(t') e^{-\sigma_n t'} \left\{ \begin{array}{c} \cos \omega_n t' \\ \sin \omega_n t' \end{array} \right\} dt' \qquad (10)$$

The excitation component of the E-pulse necessary to eradicate the response due to a preselected excitatory component can be constructed as an expansion over an appropriately chosen set of linearly independent basis functions as

$$e^e(t) = \sum_{m=1}^{M} c_m g_m(t). \qquad (11)$$

Equation (10) then becomes

$$\sum_{m=1}^{M} M_{nm}(T_e) C_m = -F_n^f, \qquad 1 \le l \le N \qquad (12)$$

Fig. 2. Decomposition of E-pulse into forcing and extinction components.

Fig. 3. Orientation for thin-cylinder excitation and first ten natural frequencies.

where

$$M_{i,m}^{c,s}(T_e) = \int_{-T_f}^{T_f} g_m(t')e^{-\sigma_i t'} \begin{Bmatrix} \cos \omega_i t' \\ \sin \omega_i t' \end{Bmatrix} dt' \qquad (13a)$$

$$F_i^{c,s} = \int_0^{T_f} e^f(t')e^{-\sigma_i t'} \begin{Bmatrix} \cos \omega_i t' \\ \sin \omega_i t' \end{Bmatrix} dt'. \qquad (13b)$$

This can be written using matrix notation as

$$\begin{bmatrix} \dfrac{M_{i,m}^c(T_e)}{M_{i,m}^s(T_e)} \end{bmatrix} \begin{bmatrix} C_1 \\ \vdots \\ C_{2N} \end{bmatrix} = - \begin{bmatrix} F_1 \\ \vdots \\ F_{2N} \end{bmatrix}. \qquad (14)$$

Solving this equation for $C_1, \cdots, C_{2N}$ determines the extinction component via (11) and thus the E-pulse.

It is convenient at this point to identify two fundamental types of E-pulses. When $T_f > 0$ the forcing vector on the right side of (14) is nonzero and a solution for $e^e(t)$ exists for almost all choices of T_e. This type of E-pulse has a nonzero excitatory component and is termed a "forced" E-pulse. In contrast, when $T_f = 0$ the forcing vector vanishes and solutions for $e^e(t)$ exist only when the determinant of the coefficient matrix vanishes, i.e., when det $[M(T_e)] = 0$. These solutions correspond to discrete eigenvalues for the E-pulse duration T_e, which are determined by rooting the determinantal characteristic equation. Since there is no excitatory component, this type of E-pulse is viewed as extinguishing its own excited field and is called a "natural" E-pulse.

IV. THIN CYLINDER E-PULSE ANALYSIS

A theoretical analysis of a thin wire target has been undertaken by various authors [11], [12]. Target natural frequencies are determined from the homogeneous solutions to the integral equation (2). The geometry of the target and its orientation with respect to the excitation field are given in Fig. 3 along with the first ten natural frequencies. The frequencies are normalized by $\pi c/L$ where L is the length of the wire and c is the speed of light, and correspond to a wire of radius given by $L/a = 200$.

The thin cylinder impulse response can be calculated by inverting (4) [12] and becomes a pure sum of natural modes in the late time. Fig. 4 shows the impulse responses of thin cylinders oriented at $\theta = 30°$ and $\theta = 60°$, generated by using the first ten modes of the target. Note the distinct early and

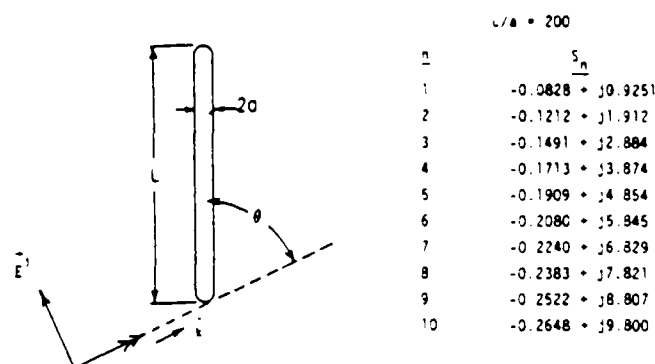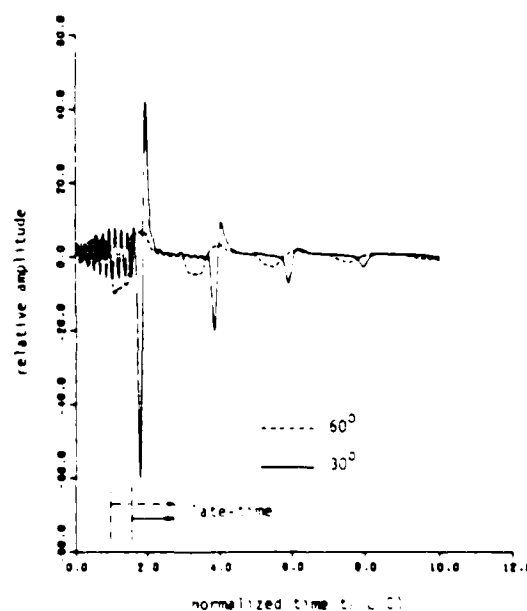Fig. 4. Thin cylinder impulse responses for $\theta = 30°$ and $\theta = 60°$ generated using the first ten natural modes.

late-time regions. An E-pulse to extinguish the first ten modes of the target is created by solving (14) using the corresponding frequencies.

Fig. 5 shows a natural E-pulse synthesized to kill the first ten natural modes of the thin wire target, using a pulse function basis set. The duration of the waveform, $T_e = 2.0408L/c$, corresponds to the first root of the resulting determinantal equation. Superimposed with this is Kennaugh's original K-pulse. The similarity is striking, with the major difference being the finite duration of the E-pulse. Also shown in Fig. 5 is a forced pulse function E-pulse constructed to extinguish the first ten modes of the target. The duration has been chosen as $T_e = 2.3$ and the excitation component has been chosen as a pulse function of width equal to that of the basis functions.

Numerical verification of the thin wire E-pulse is given in Fig. 6. The natural E-pulse waveform of Fig. 5 is convolved with the 30° and 60° impulse responses of Fig. 4 and the resulting backscattered field representations are observed to be zero in the late time. Note also the expected nonzero early time response. This portion is useful since it provides a
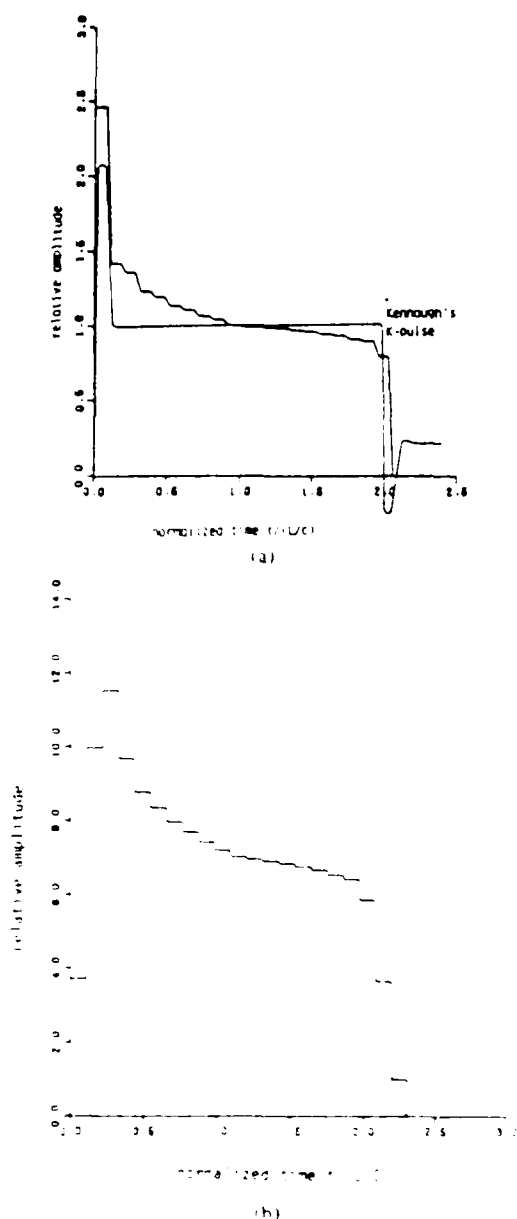
Fig 6.   Convolution of ten mode natural E-pulse with 30° and 60° ten mode impulse responses showing null late-time response.

Fig 5   Pulse function based E-pulse synthesized to eliminate first ten modes of thin cylinder target (a) Natural E-pulse compared to Kennaugh's K-pulse (b) Forced E-pulse of duration $T_e = 2.3 L/c$

comparative benchmark assessing the quality of the annulled component of the response. this is important when imperfect "extinction" is evident (due to noise, errors in the natural frequencies, etc.)

The question of E-pulse waveform uniqueness as the number of natural frequencies extinguished N is taken to infinity has not been resolved. For the thin cylinder target there appears to be such a unique waveform. Evidence is provided by Fig 7 which shows natural E-pulses of minimum duration designed to extinguish various numbers of natural modes, using both Fourier cosine and pulse function basis sets. It is apparent that these waveforms are nearly identical and they appear to be converging to a particular shape.

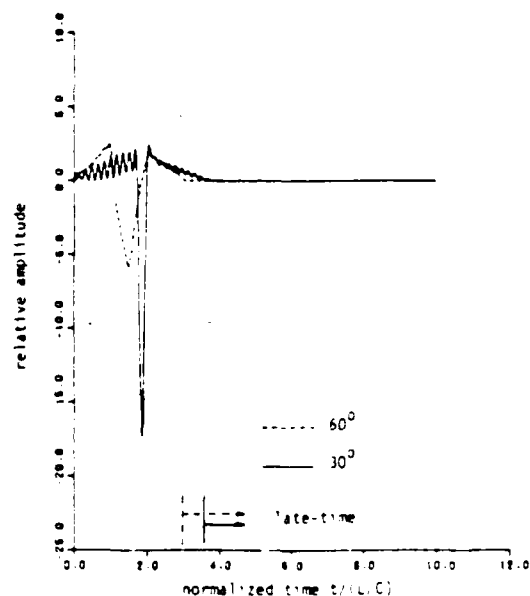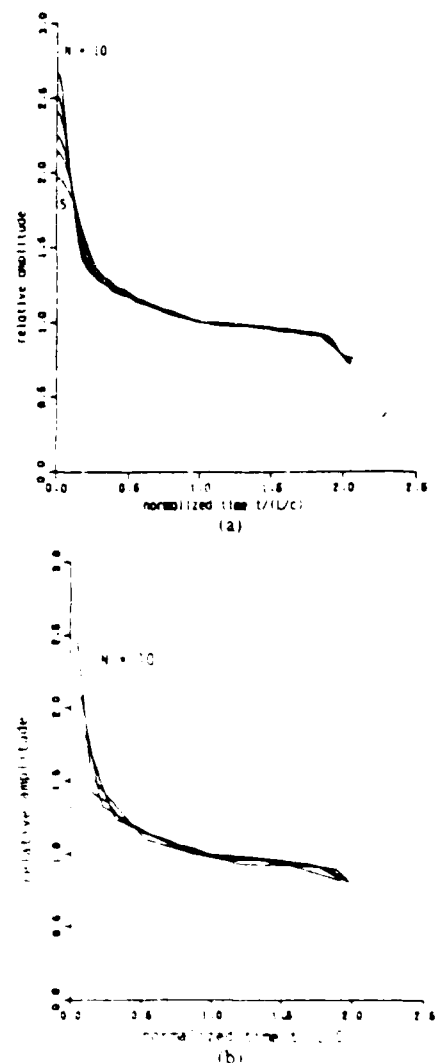The most critical parameter necessary for E pulse unique

Fig 7   Natural E pulse constructed using (a) Fourier cosine basis functions to eliminate 5, 6, 7, 8, 9, and 10 modes (b) Pulse function basis functions to eliminate 5, 6, 7, and 10 modes

ness is the finite E-pulse duration T_e. This must converge to a distinct value as $N \to \infty$. For the pulse function basis set it can be shown that the natural E-pulse durations are given by

$$T_e = 2\pi N \frac{p}{\omega_l}, \qquad p = 1, 2, \cdots, \quad 1 \leq l \leq N \qquad (15)$$

where ω_l is the imaginary part of the lth natural frequency. If this is written for the thin cylinder as

$$\omega_l = \pi [l - \delta(l)] \frac{c}{L} \qquad (16)$$

where $\delta(l)/l$ decreases asymptotically to zero with increasing l, then the minimum E-pulse duration converges to

$$(T_e)_{min} = \lim_{N \to \infty} \frac{2\pi N}{\pi [N - \delta(N)]} \frac{L}{c}$$

$$= 2\frac{L}{c}. \qquad (17)$$

V TARGET DISCRIMINATION WITH E-PULSE WAVEFORMS

Discrimination between different thin cylinder targets is demonstrated by convolving the natural E-pulse of Fig. 5, which has been constructed to extinguish the first ten modes of a target of length L, with the impulse response of the expected target and a target 5 percent longer. The result is shown in Fig. 8. The late-time response of the expected target has been successfully annulled, while the response of the differing target is nonzero over the same period. The difference in target natural frequencies provides the basis for discrimination based on the comparison of adequately dissimilar late-time responses of differing targets.

Sensitivity of E-pulse performance to the presence of uncorrelated random noise is investigated by perturbing each point of the thin cylinder impulse response of Fig. 4 by a random amount not exceeding 10 percent of the maximum waveform amplitude. The result is shown in Fig. 9. An attempt is then made to extinguish this noisy response by convolving it with the natural E-pulse of Fig. 5. As expected, the convolution, shown in Fig. 10, does not exhibit a null late-time response, but results in a distribution of noise about the zero line. Also plotted in this figure is the convolution of the E-pulse with a noisy waveform representing a target 5 percent longer. It is quite easy to separate the effects of noise and target length sensitivity, suggesting that random noise will not interfere with target discrimination.

VI EXPERIMENTAL VERIFICATION OF THE E-PULSE CONCEPT

Time domain measurements of complex conducting target responses provide the means for a practical test of the E-pulse concept. The present experiment involves measuring the near scattered field response of a simplified aircraft model to transient pulse excitation. A Tektronix 109 pulse generator is used to provide a quasirectangular 400 V incident pulse of nanosecond duration. Transmission of the pulse over a 5×6 m conducting ground screen is accomplished by using an imaged biconical antenna of axial height 2.5 m, half-angle of
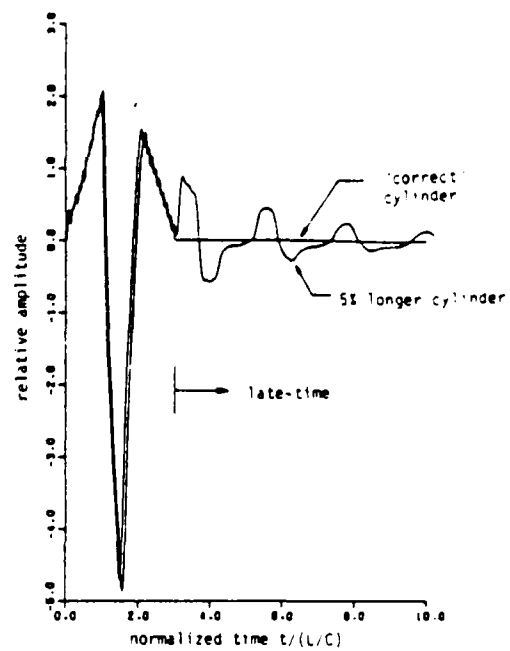

Fig. 8. Convolution of 10 mode natural thin cylinder E-pulse with 60° thin cylinder impulse response and 60° response of a cylinder 5 percent longer.
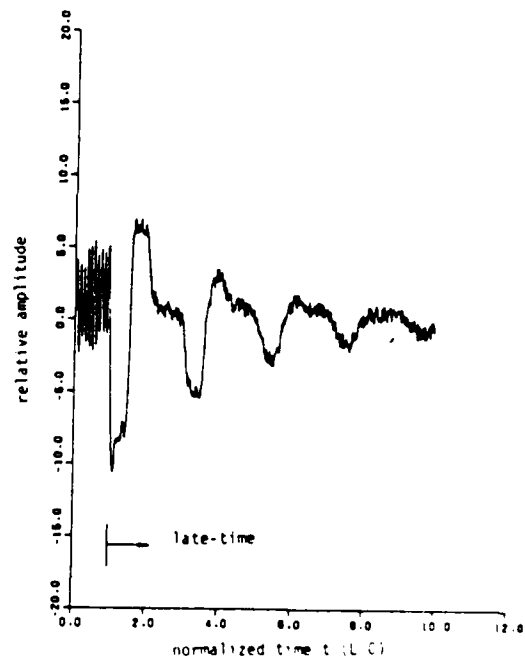

Fig. 9. Thin cylinder 60° impulse response generated from first ten natural modes, with 10 percent random noise added.

8° and characteristic impedance of 160 Ω, while reception is implemented using a short monopole E-field probe of length 1.6 cm. Although the receiving probe is not positioned in the far field region of the scatterer, the resulting measurements have the desired modal content in the late-time period, providing the small probe purely differentiates the waveform. Lastly, discrete sampling of the time domain waveform is accomplished by using a Tektronix sampling oscilloscope (S2 sampling heads, 75 ps risetime) coupled to a Radio Shack model III microcomputer.
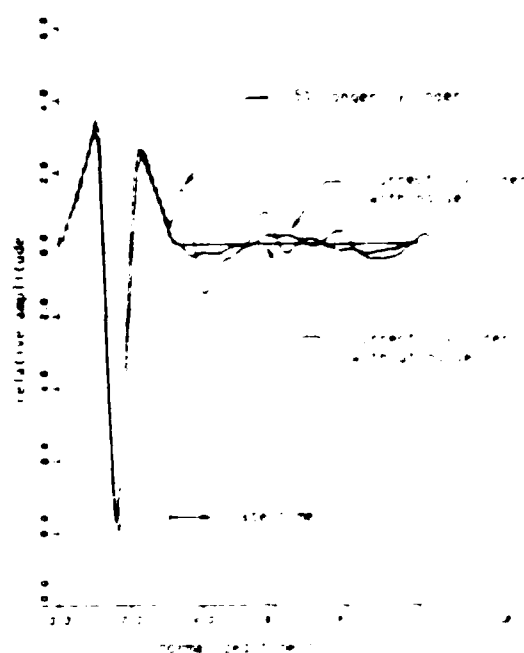
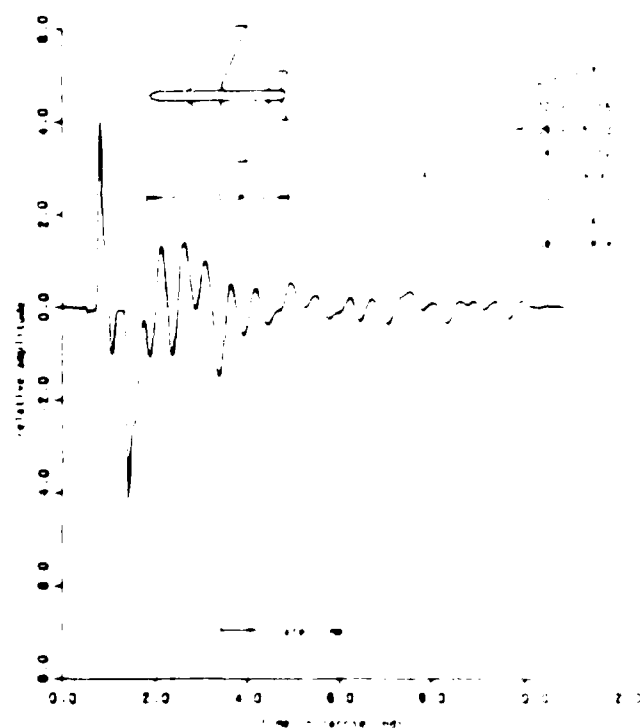Fig 10   Convolution of natural ten mode E pulse with noisy ten mode suf
impulse response

Fig 12   Measured response of a McDonnell Douglas F 18 aircraft model
and give dominant natural frequencies

Fig 11   Measured response of a Boeing 707 aircraft model and seven
dominant natural frequencies

Fig 13   Natural E pulse constructed to eliminate the seven dominant modes
in the 707 measured response

In this experiment, an attempt is made to discriminate between two aircraft models by employing the E pulse technique Figs 11 and 12 show the measured pulse responses of simplified Boeing 707 and McDonnell Douglas F 18 aircraft models, respectively Each model is constructed of aluminum and has a geometry as indicated in the figures Also shown in
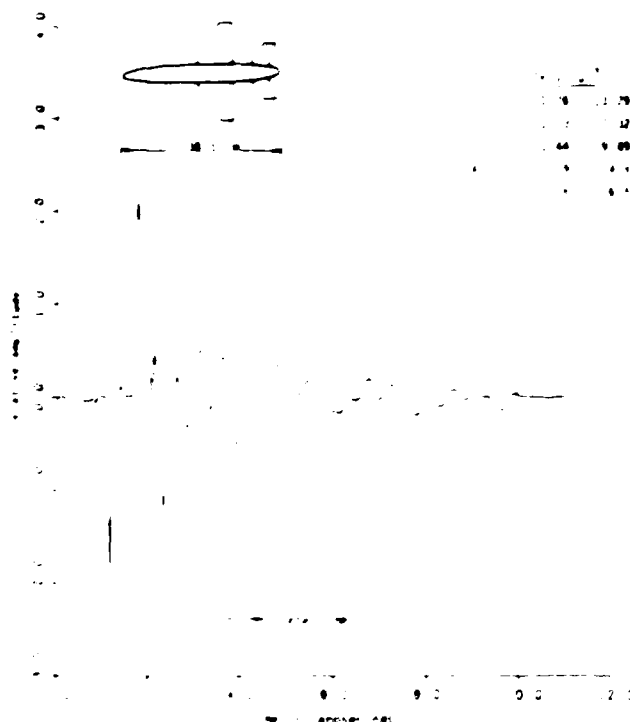
the figures are the dominant natural frequencies extracted from the late time portion of the response using a nonlinear least squares curve fitting technique [13] E pulse waveforms can then be constructed to annul these frequencies

Pulse function based natural E pulses constructed to annul each of the two target responses are shown in Figs 13 and 14 Discrimination between the targets is accomplished by convolving these waveforms with the measured responses of Figs 11 and 12 Fig 15 shows the convolution of the F 18 E pulse
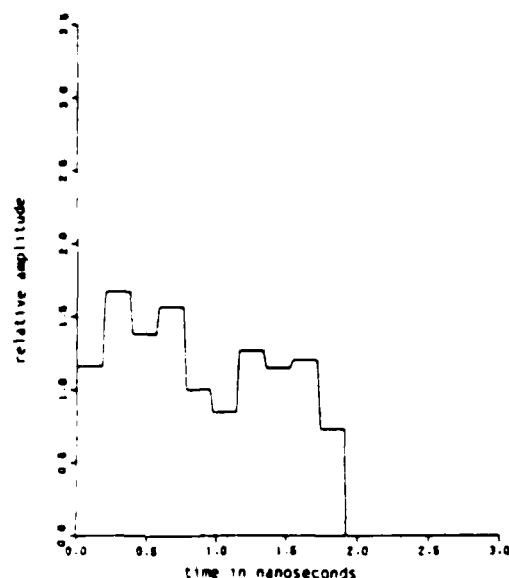
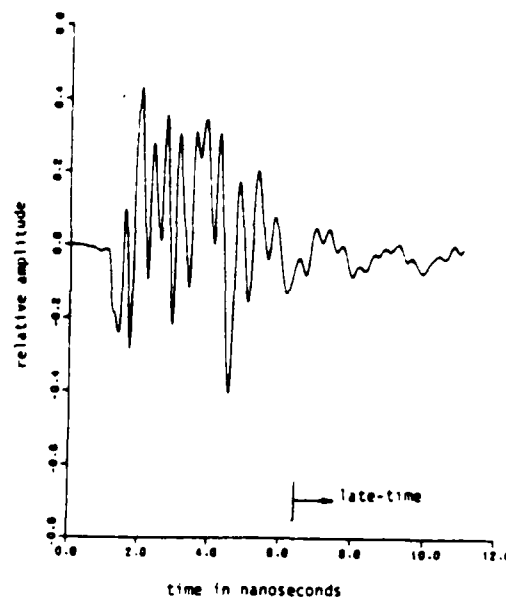Fig. 14 Natural E-pulse constructed to eliminate the five dominant modes in the F-18 measured response.

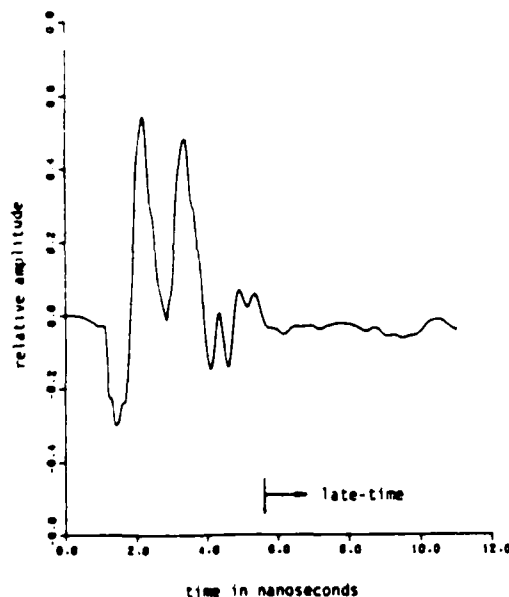Fig. 16. Convolution of the 707 E-pulse with the F-18 measured response.

Fig. 15. Convolution of the F-18 E-pulse with the F-18 measured response showing "extinguished" late-time region.
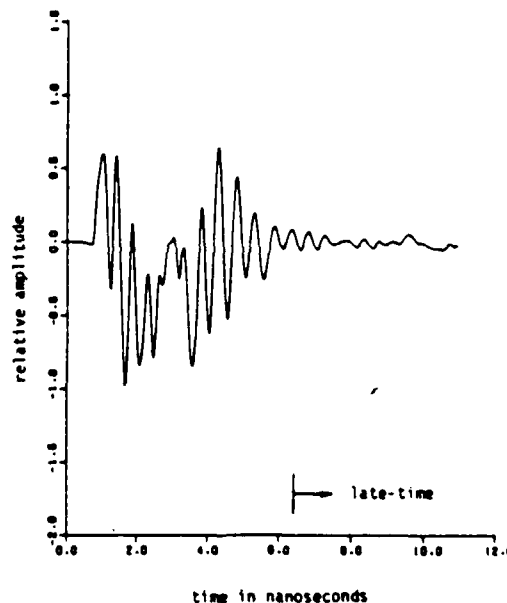

Fig. 17. Convolution of the 707 E-pulse with the 707 measured response showing "extinguished" late-time region.

with the F-18 measured response. Compared to early time, the late-time region has been effectively annulled. In contrast, Fig. 16 shows the convolution of the 707 E-pulse with the F-18 measured response. The result is a relatively larger late-time amplitude. Similarly, Fig. 17 displays the convolution of the 707 E-pulse with the 707 measured response. Again, the late-time region of the convolution exhibits small amplitude. Lastly, Fig. 18 shows the convolution of the F-18 E-pulse and the measured response of the 707 model. As before, the "wrong" target is exposed by its larger late-time convolution response.

VII. SUMMARY AND CONCLUSION

Radar target discrimination based on the natural frequencies of a conducting target has been investigated. The response of targets to a particular class of waveforms known as "E-pulses" has been demonstrated to provide an effective means for implementing a discrimination process in the presence of random noise.

Two types of E-pulses have been identified, natural and forced. Discrimination based on natural E-pulses and the response of a thin cylinder target has been demonstrated theoretically.
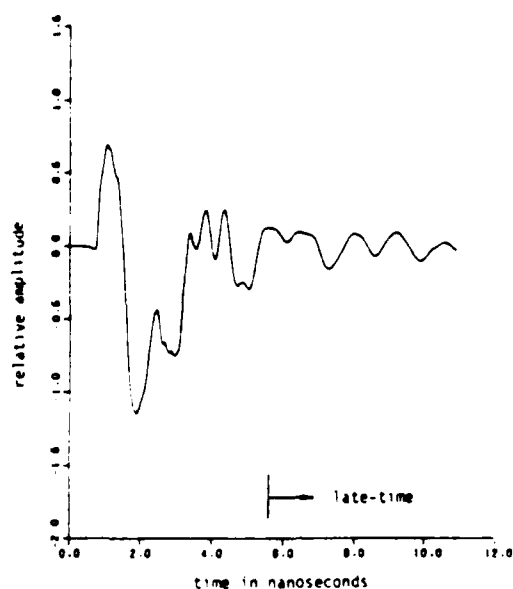
Fig. 18. Convolution of the F-18 E-pulse with the 707 measured response.

Most encouraging are the experimental results which reveal that two quite complicated, similar sized targets can be adequately and convincingly discriminated using natural E-pulse waveforms. Further experimentation using more accurate aircraft models is currently being undertaken.

REFERENCES

[1] K. M. Chen, "Radar waveform synthesis method—a new radar detection scheme," IEEE Trans. Antennas Propagat., vol. AP-29, no. 4, pp. 553-566, July 1981.

[2] D. L. Moffatt and R. K. Mains, "Detection and discrimination of radar targets," IEEE Trans. Antennas Propagat., vol. AP-23, no. 3, pp. 358-367, May 1975.

[3] A. J. Berni, "Target identification by natural resonance estimation," IEEE Trans. Aerospace Electron. Syst., vol. AES-11, no. 2, pp. 147-154, Mar. 1975.

[4] C. W. Chuang and D. L. Moffatt, "Natural resonances of radar targets via Prony's method and target discrimination," IEEE Trans. Aerospace Electron. Syst., vol. AES-12, no. 5, pp. 583-589, Sept. 1976.

[5] E. M. Kennaugh, "The K-pulse concept," IEEE Trans. Antennas Propagat., vol. AP-29, no. 2, 327-331, Mar. 1981.

[6] C. E. Baum, "The singularity expansion method," in Transient Electromagnetic Fields, L. B. Felsen, Ed. New York: Springer-Verlag, 1976, ch. 3, pp. 129-179.

[7] M. A. Morgan, "Singularity expansion representation of fields and currents in transient scattering," IEEE Trans. Antennas Propagat., vol. AP-32, no. 5, pp. 466-473, May 1984.

[8] L. W. Pearson, "A note on the representation of scattered fields as a singularity expansion," IEEE Trans. Antennas Propagat., vol. AP-32, no. 5, pp. 520-524, May 1984.

[9] K. M. Chen and D. Westmoreland, "Radar waveform synthesis for exciting single-mode backscatter from a sphere and application for target discrimination," Radio Sci., vol. 17, no. 3, pp. 574-588, May-June, 1982.

[10] C. E. Baum, "Emerging technology for transient and broad band analysis of antennas and scatterers," Proc. IEEE, vol. 64, no. 11, pp. 1598-1616, Nov. 1982.

[11] K. M. Chen et al., "Radar waveform synthesis for single-mode scattering by a thin cylinder and application for target discrimination," IEEE Trans. Antennas Propagat., vol. AP-30, no. 5, pp. 867-880, Sept. 1982.

[12] F. M. Tesche, "On the analysis of scattering and antenna problems using the singularity expansion technique," IEEE Trans. Antennas Propagat., vol. AP-21, no. 1, pp. 53-62, Jan. 1973.

[13] B. Drachman and E. Rothwell, "A continuation method for identification of the natural frequencies of an object using a measured response," IEEE Trans. Antennas Propagat., vol. AP-33, no. 4, pp. 445-450, Apr. 1985.

A Continuation Method for Identification of the Natural Frequencies of an Object Using a Measured Response

BYRON DRACHMAN AND ED ROTHWELL, STUDENT MEMBER, IEEE

Abstract—The identification of the natural frequencies of an object using measured data is an ill-conditioned problem. A method and algorithm to solve the problem based on regularization by a continuation method is presented. The algorithm is applied to the measured response of a model aircraft, and the superiority of this method to Prony's method in the presence of noise is demonstrated.

I. INTRODUCTION

The singularity expansion method (SEM) [2] advocates representing the late-time electromagnetic field scattered from a finite sized conducting body as a sum of damped sinusoids (natural modes). An important problem is to extract the natural frequencies $s = \sigma + j\omega$ from a time domain measurement of such a scattered field. We desire to find a function of the form

$$F(A_1, \cdots, \psi_N, K, t) = K + \sum_{n=1}^{N} A_n e^{\sigma_n t} \cos(\omega_n t + \psi_n) \quad (1)$$

which "best fits" in some way the measured data. This problem is known to be ill-conditioned [11] and the straightforward use of nonlinear least squares or Prony's method is unreliable. We present a method of solving this problem via a regularization process—changing the ill-conditioned problem into a well-conditioned one with a sufficiently similar solution.

Our goal is to give an overview of the mathematical basis for this method and a usable, easily understood algorithm for its implementation. More detailed analyses and more elaborate algorithms can be found in the cited references.

II. ILL-CONDITIONED PROBLEMS

Consider a problem and an algorithm to solve the problem. When data are applied to the algorithm a solution results. If a small change in the data leads to a relatively large change in the computed solution, the process of obtaining the solution is termed "ill-conditioned." In matrix theory, the conditioning leading to the solution of the equation $Ax = b$ is described by the condition number of the matrix A, which can be calculated directly using singular value decomposition (SVD), or estimated [5]

It is important to distinguish between an ill-conditioned algorithm and an ill-conditioned problem. If the problem is ill-conditioned then no algorithm will work well enough to produce accurate results (Rice [11, p. 111]). The extraction of natural frequencies from a measured target response is such a problem.

"Regularization" is a technique for solving an ill-conditioned problem by transforming it into a related well-conditioned problem with a solution that is a good approximation to the elusive

solution of the original problem. See Phillips [9], Tikhonov [15], Rice [11], and Nashed [7] for more rigorous definitions and discussions. Our choice for a regularization scheme is to use a continuation method.

III. THE CONTINUATION METHOD

Let $\vec{F}(\vec{x})$ be a nonlinear vector valued function of the vector $\vec{x}$. Solving the problem $\vec{F}(\vec{x}) = 0$ by Newton's method or a quasi-Newton method requires a good initial guess for convergence [13]. The conventional continuation method may be viewed as a numerical technique to overcome this difficulty. Instead of solving $\vec{F}(\vec{x}) = 0$, construct a family of functions

$$G_\tau(\vec{x}) = \tau\vec{F}(\vec{x}) + (1 - \tau)(\vec{x} - \vec{x}^0), \qquad 0 \leqslant \tau \leqslant 1 \qquad (2)$$

where $\vec{x}^0$ is an initial guess for the solution to $\vec{F}(\vec{x}) = 0$, and solve the series of problems $\tau = 0, \tau_1, \cdots, \tau_f = 1$. In an iterative procedure, $\tau = \tau_i$ is replaced by $\tau_{i+1} = \tau_i + \Delta\tau_i$ and the problem $\vec{G}_{\tau_{i+1}}(\vec{x}) = 0$ is solved for $\vec{x} = \vec{x}^{i+1}$ using $\vec{x}^i$ as an initial guess (where it is assumed that $\Delta\tau_i$ is small enough to insure convergence). The process is begun with $\tau = 0$, $\vec{x} = \vec{x}^0$ and proceeds to $\tau = \tau_f = 1$ and the desired solution to $\vec{F}(\vec{x}) = 0$.

If the original problem $\vec{F}(\vec{x}) = 0$ is ill-conditioned, we choose to view the continuation method as a regularization procedure. The problem $\vec{x} - \vec{x}^0 = 0$ determined by $\tau = 0$ is well-conditioned, while $\tau = 1$ corresponds to the original ill-conditioned problem. Regularization is then accomplished by making τ as close to one as possible to adequately approximate the solution to $\vec{F}(\vec{x}) = 0$ while keeping enough of the well-conditioned term $(\vec{x} - \vec{x}^0)$ to keep the combined problem well-conditioned.

Theorems concerning sufficient conditions for the convergence of the continuation method are discussed in [8] and [4]. Allgower and Georg [1] also give a survey and history of the continuation method.

IV. IDENTIFICATION OF NATURAL FREQUENCIES BY A CONTINUATION METHOD

We wish to obtain a best fit to the sampled late-time target response $\{\vec{r}_i = \vec{r}(t_i)\}$ by minimizing

$$\sum_i [\vec{F}(\vec{x}, t_i) - \vec{r}_i]^2 \qquad (3)$$

where $\vec{F}(\vec{x}, t)$ is the fitting function given by (1) and $\vec{x} = (A_1, \sigma_1, \cdots, \omega_N, \psi_N, K)^T$ is a vector containing the unknown amplitudes, natural frequencies, and phases of the natural modes, and the dc level. Consider $\vec{f}(\vec{x})$ as a vector valued function with ith component $\vec{F}(\vec{x}, t_i)$ and $\vec{R}$ a column vector with ith component $\vec{r}_i$. Minimizing (3) then corresponds to minimizing $\|\vec{f}(\vec{x}) - \vec{R}\|^2$ (L_2 norm). This problem is ill-conditioned, but can be regularized by applying the continuation method and minimizing

$$\tau\|\vec{f}(\vec{x}) - \vec{R}\|^2 + (1 - \tau)\|\vec{x} - \vec{x}^0\|^2 \qquad (4)$$

where $\vec{x}^0$ is an initial guess. It is assumed that $\vec{x}$ and $\vec{x}^0$ are appropriately normalized dimensionless quantities. With τ fixed, differentiation of (4) with respect to the variables in $\vec{x}$ yields the normal equation

$$\vec{H}(\vec{x}, \tau) = \tau(\text{grad}_{\vec{x}}\vec{f})(\vec{f} - \vec{R}) + (1 - \tau)(\vec{x} - \vec{x}^0) = 0 \qquad (5)$$

where $\text{grad}_{\vec{x}}\vec{f}$ is the transpose of the Jacobian matrix of $\vec{f}$.

We assume that (5) determines a simple path in $(\vec{x}, \tau)$ space leading from $(\vec{x}^0, \tau_0)$ to $(\vec{x}^f, \tau_f)$, as shown in Fig. 1. If the path
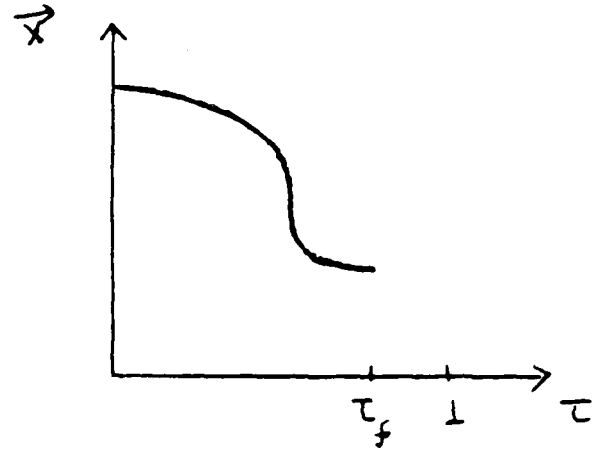

Fig. 1. Typical path in (x, τ) space.

is parameterized by arc length s and the chain rule is applied to (5), we have

$$\frac{d}{ds}\vec{H}(\vec{x}(s), \tau(s))$$

$$= (\text{grad}_{\vec{x}}\vec{H}) \cdot \frac{d\vec{x}}{ds} + \frac{d\vec{H}}{d\tau}\frac{d\tau}{ds} = 0. \qquad (6)$$

This is viewed as a differential equation

$$\begin{pmatrix} \dfrac{d\vec{x}}{ds} \\ \dfrac{d\tau}{ds} \end{pmatrix} = \vec{\nu} \qquad (7)$$

where $\vec{\nu}$ is a normalized solution to the homogeneous equation

$$\left(\text{grad}_{\vec{x}}\vec{H}, \frac{d\vec{H}}{d\tau}\right)\vec{\nu} = 0. \qquad (8)$$

If we assume that at each point on the curve

(a) $\left(\text{grad}_{\vec{x}}\vec{H}, \dfrac{d\vec{H}}{d\tau}\right)$ has full rank

(b) $A(s) = \begin{pmatrix} \left(\dfrac{d\vec{x}}{ds}\right)^T, \dfrac{d\tau}{ds} \\ \text{grad}_{\vec{x}}\vec{H}, \dfrac{d\vec{H}}{d\tau} \end{pmatrix}$ is nonsingular

then (7) can be solved using a standard ODE follower. We can also construct a "predictor-corrector" follower to step along the path until the final point $(\vec{x}^f, \tau_f)$ is reached, either at $\tau_f = 1$ or when the problem becomes too ill-conditioned. The predictor step (Euler) is to solve (8) for $(\Delta\vec{x}, \Delta\tau)$ with a prechosen value of Δs. The sign of det $(A(s))$ is used to choose the correct sign of $\vec{\nu}$; that is, to continue moving in the same direction along the curve. If $A(s)$ becomes singular (indicating self-crossings or bifurcations of the path) see Keller [4] for more advanced techniques. Also Allgauer and Georg [1] give details for incorporating variable step size Δs.

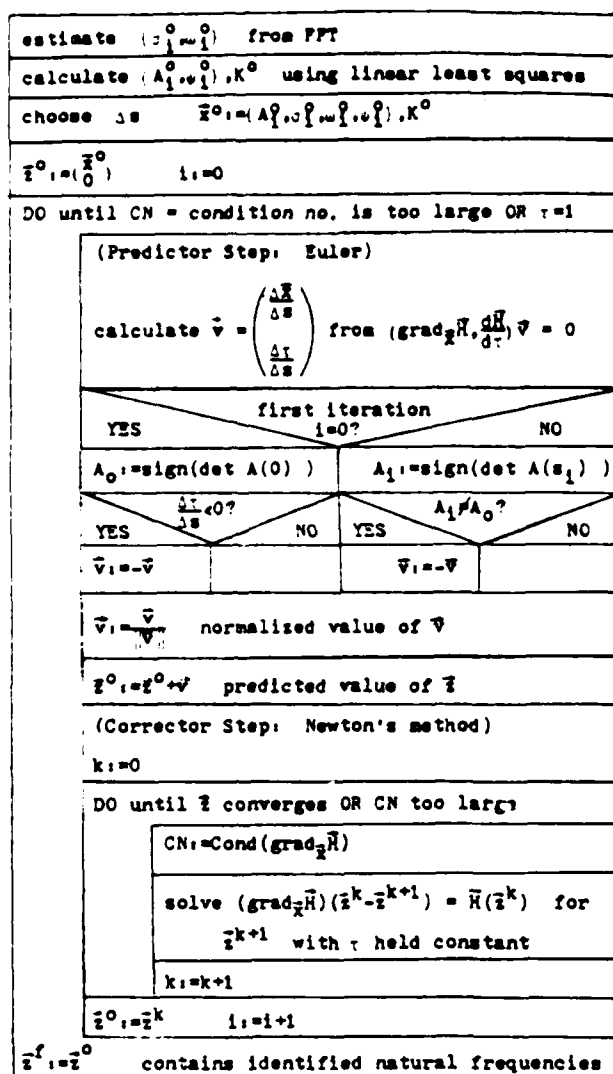Correction back to the curve uses Newton's method with τ he

Fig. 2.   Flowchart for continuation method.

constant. The condition number of $(\text{grad}_{\bar{z}} \vec{H})$ is computed using SVD at each step to test for termination of the algorithm. (We used a CDC 750 which carries 13 digits, assumed three digits of accuracy in the measured data, and terminated when the condition number exceeded 10^{10}.) Allgower and Georg [1] contains an alternate method for correction.

At termination the identified natural frequencies are contained in $\bar{x}^f$. A flowchart for our algorithm is shown in Fig. 2.

V. EXPERIMENTAL AND NUMERICAL RESULTS

The first example is shown in Fig. 3 and demonstrates the advantage of using the continuation method over Prony's method in the presence of random noise. The theoretical impulse response of a thin wire at a $30°$ aspect angle has been computed by SEM using the first eight natural frequencies [14], [2]. This is shown in Fig. 3(a). Fig. 3(b) shows the same reponse with 10 percent random noise added (10 dB max signal/max noise). Fig. 3(c) displays the natural frequencies extracted from the noisy response using the continuation method and Fig. 3(d) by Prony's method. Clearly in this example the continuation method yields more accurate results. Further refinements of Prony's method are avail-

able (such as overguessing the number of modes and averaging [6], [10]), but we have never obtained results as good as those obtained from the continuation method.

The second example uses the measured pulse response of a Boeing 707 aircraft model as seen in Fig. 4(a). Fig. 4(b) shows the Fourier transform (via fast Fourier transform (FFT)) of the late-time portion of the measured response. The seven largest peaks were used to determine initial guesses for ω_i, $1 \leq i \leq 7$, in the continuation method. The resulting best fit to the late time is shown in Fig. 4(c). The experimental set-up yielding Fig. 4(a) is described in [16].

VI. DISCUSSION

The numerical evidence shows the superiority of regularization via a continuation method over Prony's method in the presence of random noise. Further numerical experimentation [12] has also shown that, in contrast to Prony's method, underestimating the number of modes in the response is not a computational disaster. In fact, it is possible to underestimate the number of modes at first, and use those results as initial guesses when solving the problem with more modes assumed. Other benefits include di-
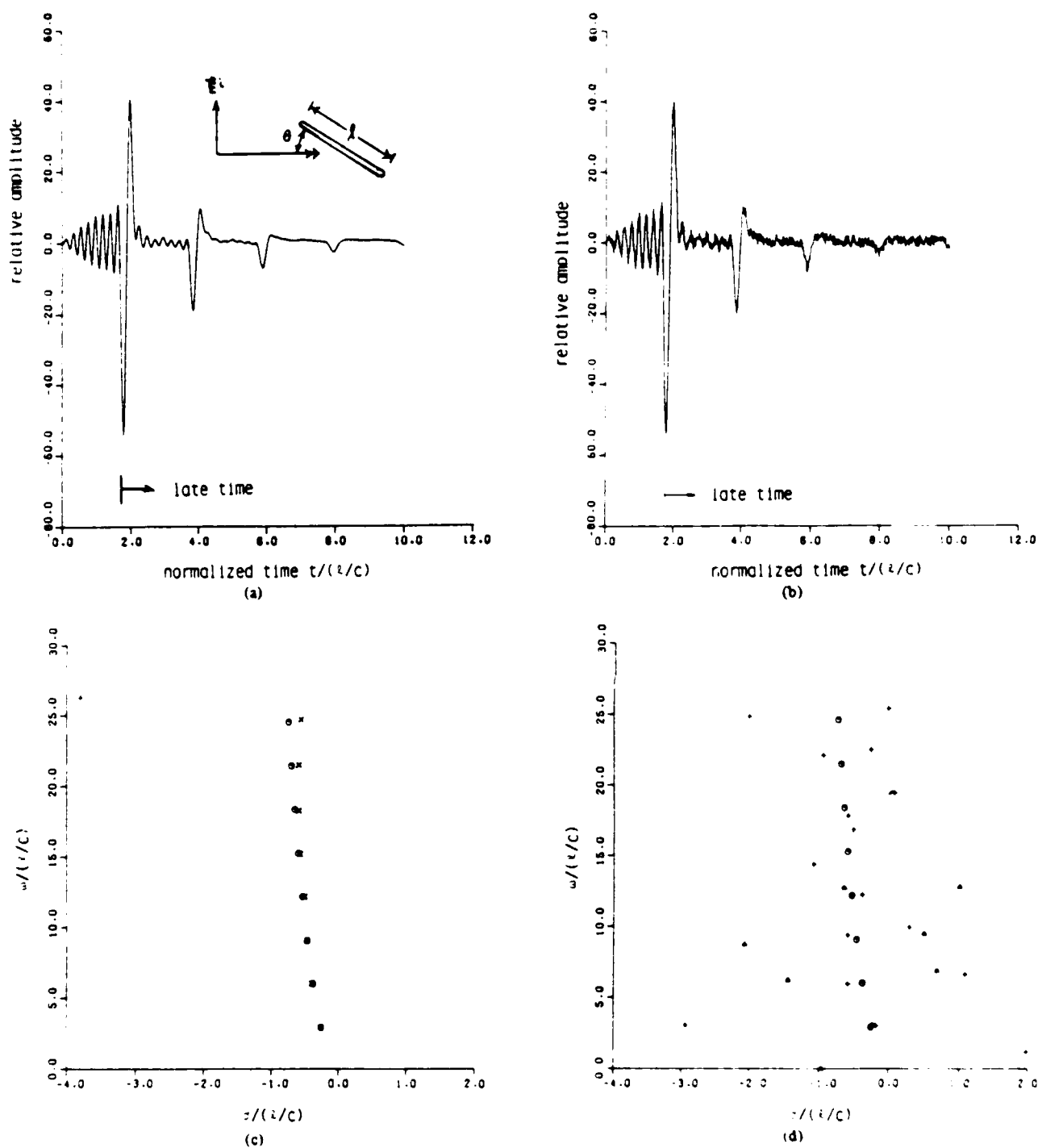
Fig. 3. (a) Theoretical impulse response of a thin wire target inclined at $\theta = 30°$, constructed using the first eight natural frequencies. (b) Thin wire impulse response with 10 percent (of maximum signal) random noise added. (c) Natural frequencies extracted from the noisy response using the continuation method. 0 exact values, x extracted values. (d) Natural frequencies extracted from the noisy response using Prony's method. 0 exact values, △ extracted values using eight modes, + extracted values using 16 modes.
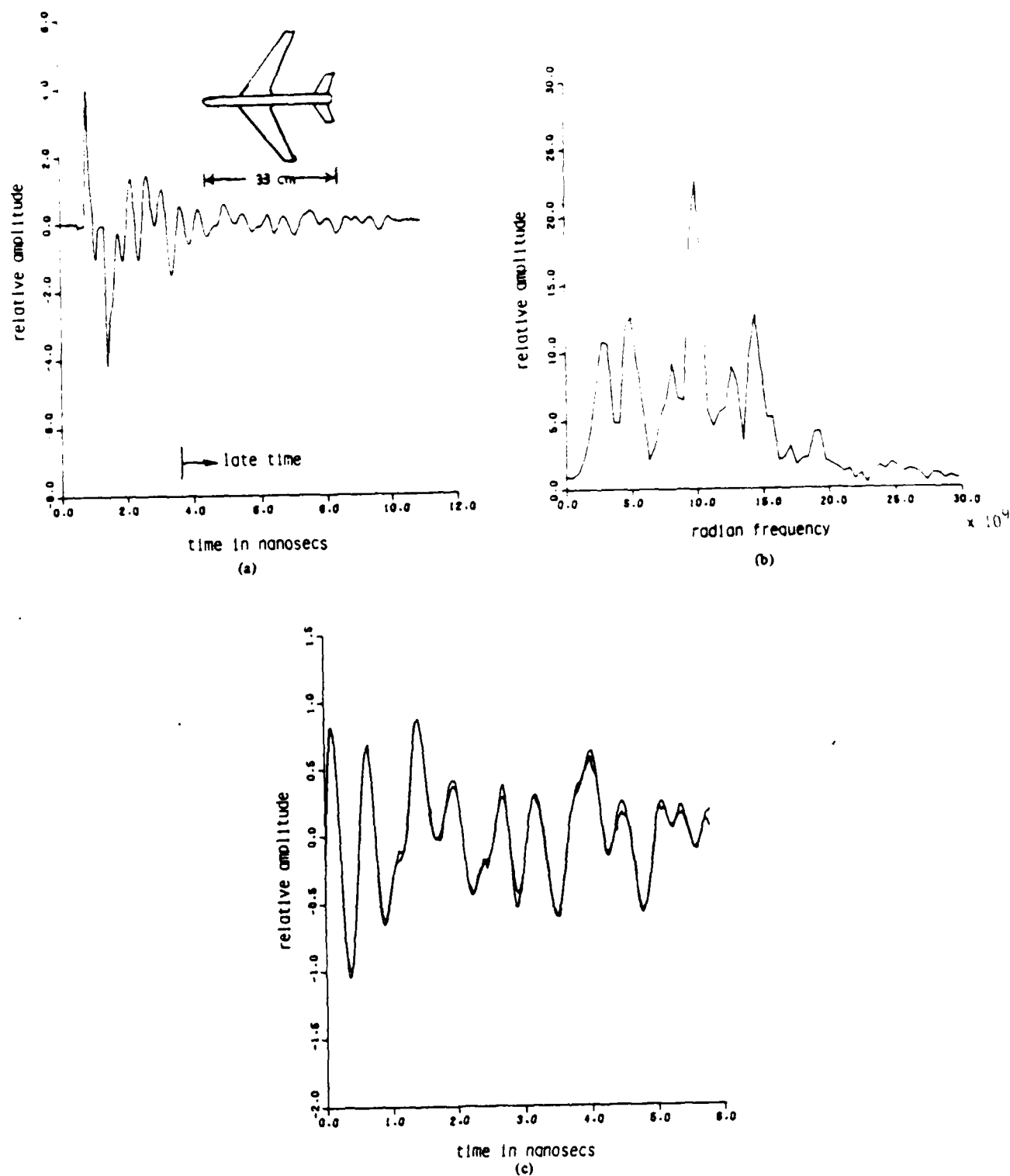
Fig. 4. (a) Measured near-field response of a Boeing 707 aircraft model to a nanosecond pulse. (b) Fourier transform of measured 707 response showing seven dominant natural modes (peaks). (c) Seven mode best fit from continuation method to late time portion of 707 response.

rectly incorporating a dc level, and the fact that overguessing the number of modes present merely results in negligible amplitude for modes not in the response

ACKNOWLEDGMENT

We wish to thank Professors Chen and Nyquist for very helpful conversations on these matters

REFERENCES

[1] Allgower and Georg, "Simplicial and continuation method for approximating fixed points and solutions to systems of equations," SIAM Rev, vol 22, no 1, Jan 1980

[2] Baum, "The singularity expansion method," in Transient Electromagnetic Fields, L B Felson. Ed New York Springer-Verlag 1976 ch 3

[3] Hildebrand, Introduction to Numerical Analysis New York McGraw Hill 1956

[4] H B Keller "Numerical solutions of bifurcation and nonlinear eigenvalue problems," in Applications of Bifurcation Theory, P Rabinowitz Ed New York Academic 1977 pp 159-384

[5] Linpack Users Guide, SIAM Philadelphia 1980

[6] E K Miller "Prony's method revisited," Lawrence Livermore Lab Rep, Oct 1978

[7] Nashed, "Operator-theoretic and computational approaches to ill posed problems with applications to antenna theory," IEEE Trans Antennas Propagat, vol AP-29, no 2, pp 220-231 Mar 1981

[8] Ortega and Rheinboldt, Iterative Solutions of Nonlinear Equations in Several Variables New York Academic 1970

[9] Phillips "A technique for the numerical solutions of certain integral equations of the first kind," ACM, vol 8-9 pp 84-89 1961

[10] Poggio Van Blancum Miller and Mittra, "Evaluation of a processing technique for transient data," IEEE Trans Antennas Propagat vol AP 26 no 1 pp 165 173 Jan 1978

[11] Rice, Matrix Computations and Mathematical Software New York McGraw-Hill 1981

[12] Rothwell and Drachman "Use of a continuation method for the extraction of natural frequencies from a target response Experimental and numerical results," presented at Nat Radio Sci Meeting Boston, June 1984

[13] Stoer and Bulirsch, Introduction to Numerical Analysis New York Springer-Verlag, 1980

[14] Tesche, "On the analysis of scattering and antenna problems using the singularity expansion method," IEEE Trans Antennas Propagat vol AP-21 pp 53-62 Jan 1973

[15] Tikhonov and Arsenin, Solutions of Ill-Posed Problems New York Wiley, 1977

[16] C Chuang, "Transient waveform synthesis for radar target discrimination," Ph D dissertation, Michigan State Univ 1981

END

5-87

DTIC